

Extreme temperature, wind and bushfire weather projections using a standardised method

Technical Report – June 2021

Authors: Andrew Dowdy¹, Andrew Brown¹, Acacia Pepler¹, Marcus Thatcher², Tony Rafter², Jason Evans³, Harvey Ye¹, Chun-Hsu Su¹, Samuel Bell¹ and Christian Stassen¹

¹Bureau of Meteorology, Docklands, Australia

²CSIRO Oceans and Atmosphere, Aspendale, Australia

³University of New South Wales, Sydney, Australia

Acknowledgements: This research was funded through the Energy Sector Climate Information (ESCI) project supported by the Australian Government, Bureau of Meteorology (BoM), CSIRO and AEMO. The authors would like to thank Chiara Holgate (BoM) and Justin Peter (BoM) for providing reviews on earlier versions of this report as well as others in the ESCI team for contributing to various aspects around the information covered in this report, including Ben Jones (AEMO), Ian Watterson (CSIRO), Chi-Hsiang Wang (CSIRO) and Leanne Webb (CSIRO).

Abstract The influence of anthropogenic climate change on extreme temperatures, winds and bushfire weather in Australia is assessed here. These assessments consider a comprehensive range of factors including based on observations, modelling and physical process understanding. Those factors are reviewed using a standardised method to collate lines of evidence for guiding the production of projections information and confidence assessment. Projections are produced using calibrated data from global and regional climate models for temperature and fire weather, with environmental diagnostics used for severe convective winds from thunderstorms. Projections include maps throughout Australia corresponding to the 10-year average recurrence interval (ARI) which is more extreme than previously presented for fire weather and severe wind projections, such that care taken to document and communicate uncertainties, supported by the comprehensive reviews and lines of evidence. A focus of the discussion is on southern and eastern Australia during summer, due to a need for this in energy sector risk assessments, but with these nationally consistent projections intended to be used more broadly for other purposes too. The results for 10-year ARI values in southern and eastern Australia during summer show increases for temperature (*Very High Confidence*), severe winds (*Low Confidence*) and bushfire weather (*High Confidence* in southern Australia; *Medium Confidence* in eastern Australia) due to increasing greenhouse gas emissions.

1. Introduction and overview

This document presents climate projections for extremes based on applying a standardised method designed to provide enhanced information on the likelihood of projected changes. The method considers a comprehensive range of lines of evidence, including from observations, reanalyses, modelling and physical process understanding. It is intended to help provide guidance around future changes in extremes, given that considering many lines of evidence can be helpful for this, including due to the range of uncertainties that often exist around projected future changes in extremes. This method is used here together with a new set of calibrated climate projections data produced for Australia, based on several regional modelling approaches for dynamical downscaling.

The method (referred to here as the standardised method for projections likelihood, SMPL) can be applied for an individual weather variable and region, or for a multivariate/compound event (e.g., relating to bushfire risk factors based on considering a range of different processes). A previous study provides examples of how this type of method can be applied for one weather variable (mean rainfall) in four individual seasons (Dowdy et al. 2015). The method is applied here for the following three variables with a focus on summer (December to February), selected based on discussions with stakeholders on key needs for the energy sector (noting the support for this research through the Energy Sector Climate Information, ESCI, project):

- extreme temperature, based on daily maximum air temperature at a height of 2 m (Section 3)
- extreme wind, based on 3 second average wind gust speed at a height of 10 m (Section 4)
- extreme bushfire weather, based on a compound event type of framework to consider a range of different risk factors (Section 5)

For some planning and design activities relating to future climate change, decisions will often need to be made regardless of whether highly confident projections are available or not. Consequently, there may be benefits in scientists providing information on projections even if those projections are not highly confident, as can be the case for some extreme events, as long as the degree of uncertainty is assessed and communicated when those projections are provided. The projections of extremes presented here are intended to help underpin such decisions, based on considering a broad range of lines of evidence.

The examination of various lines of evidence is intended to help guide the selection of data and methods for providing projections to end users, as well as to help produce confidence assessment information to accompany the provision of those projections. For example, examining the lines of evidence for a specific purpose (e.g., projections of extremes for energy sector needs in southeast Australia) can help provide guidance when producing the projections on whether a particular modelling approach could be useful to include or not (or perhaps weighted differently within a broader ensemble of datasets). That type of targeted guidance can be used together with other more general sources of guidance relevant to projections data selection, such as based on broader assessments of models and methods relating to climate change projections such as presented by CSIRO & BoM (2015) as well as in the ESCI project technical report on modelling and downscaling (Thatcher et al. 2021).

The lines of evidence are also intended for use when producing confidence assessment information in the projections. The confidence assessment information can include measures such as ranges of change (e.g., probabilistic estimates of likely ranges that may be above, or

below, the most likely estimate for the projected change) and other approaches such as descriptive terms for communicating the degree of confidence (e.g., words with quantitative probabilities associated with them such as those used for IPCC (Mastrandrea et al. 2011)).

For information on the likelihood of projected future changes in these weather-related variables, stakeholder feedback recommended a focus on extremes corresponding to the 10-year average recurrence interval (ARI), representing an event with a return period of 10 years on average (noting that the return period is equal to the reciprocal of the annual probability of exceedance). Maps of the most likely future projected change in values corresponding to the 10-year ARI were requested by stakeholders for these weather-related variables, together with estimates of the 10th and 90th percentile range of plausible values as a confidence assessment measure. Maps of those quantities are presented in later parts of this report, based on considering various lines of evidence. The resultant maps (and data layer for each of those maps) are intended for use such as by risk analysts in the energy sector as well as for a broader range of user groups including in other sectors. The lines of evidence are not intended to be of direct use by risk analysts but are provided to document the method used and the supporting science details.

The following Section 2 describes the steps for applying the method, then provides some examples of practical uses of the outputs for improved resilience to climate hazards. Sections 3-5 document the application of the method for extreme temperatures, winds and fire weather, respectively. The outputs from the application of this method include national maps and data files of 10-yr ARI values (available on request), with supporting review summaries and confidence information.

2. Description of method and implementation of results

2.1 Steps used to apply the method

Applying the method consists of two steps, referred to here as producing the Lines of Evidence Table (Step 1) and then producing the Projections Likelihood Information (Step 2). The method is applied individually for each variable of interest (e.g., extreme temperature, extreme wind and extreme fire weather are the three variables considered here). For this study, the Projections Likelihood Information includes maps showing the most probable change in values corresponding to the 10-year ARI, together with estimates of the 10th and 90th percentile range of plausible change.

Step 1 – Produce the Lines of Evidence Table

- Collect a wide range of information on climate change that could be of relevance to consider when populating the Lines of Evidence Table. This information could be obtained from new analyses as well as from a review of existing literature. The information could consider aspects such as observations, reanalyses, model data and physical process understanding. For example, relevant information could potentially include analysis of long-term observed trends, model simulations of future climate, uncertainties in observations, uncertainties relating to a modelling approach's ability to simulate physical processes and observed features (such as the seasonal cycle or spatial detail of extremes), as well as the influence of large-scale drivers (e.g., ENSO, IOD and SAM) in the historical and future projected climates.
- Collate that information into short text summaries on different topics, with accompanying figures and references provided to support these summaries, aiming for a general balance of evidence based on the available science. The summaries can be grouped into broader categories: e.g., physical processes, historical information and projected changes (as also used for the broad sections of the Lines of Evidence Table).
- Use those short text summaries to populate the Lines of Evidence Table. This table contains a different row for each of the different aspects being considered (e.g., observed trends could be on one row of the table, with modelled trends on another row of the table), with examples of these tables provided in Section 3-5 as well as in a previous application for rainfall in eastern Australia (Dowdy et al. 2015). For each aspect being considered, the collected information is used to provide two key details: the degree of influence that this aspect has on the variable in the region being considered; and what this implies for the direction of projected future change (either an increase, decrease, little change or increased uncertainty). This is intended as a standardised way to synthesise a broad range of information for this method.

Step 2 – Produce the Projections Likelihood Information

- For the projected change of interest (e.g., here we consider the change from the historical period to a future period in values corresponding to the 10-year ARI), use the Lines of Evidence Table to determine the best available data and methods for estimating a given likelihood measure. For example, here we aim to produce the most probable projected change, together with estimates of the 10th and 90th percentile range of plausible change. The method to determine the best available estimate for a given likelihood measure may vary between different weather variables of interest (e.g., depending on the degree of confidence in models to simulate relevant physical processes). For example, this variation could include the selection of different datasets and methods (e.g., the use of direct model

output or statistical diagnostic methods) or scaling some data differently in a model ensemble.

- For quantities that have a reasonably robust range of evidence, with good agreement between those different lines of evidence (e.g., about two thirds of the Lines of Evidence Table having a consistent sign of future change), then model output may be the best option for producing the Projections Likelihood Information, while still considering the various uncertainties and strengths/weaknesses of different modelling approaches for helping to guide the production of the data products. For quantities with lower confidence (i.e., limited evidence and/or low agreement between lines of evidence), then a more qualitative best estimate could be appropriate. For example, in some cases with very high uncertainty the best estimate for the Projections Likelihood Information might simply be ‘an increase is more likely than a decrease’ for a particular region, if that is the best information that can be provided based on the balance of available knowledge from the Lines of Evidence Table. It is acknowledged that given the broad range of different information sources and data types (e.g., direct model output or statistical diagnostic methods) this step of the process may require some degree of expert judgement to be used.
- The Projection Likelihood Information can include confidence assessment information, such as based on the degree of evidence and agreement from the Lines of Evidence table. Here we use the estimates of the 10th and 90th percentile range of plausible change for indicating the degree of confidence in the projected future changes as well as noting other approaches that can be used for some applications, including the framework shown in Table 2.1 together with words that have quantitative probabilities associated with them to accompany the provision of projections.

Additional details on the method

In addition to maps for 10-year ARI values, which is the focus of the application examples presented here, it is possible to produce the Projections Likelihood Information for individual locations or for regional averages. That form of information could be used to populate a table for different locations or regions. It could also be done for different magnitudes of a particular quantity of interest, such as the likelihood of wind speeds in the range 20-30 m.s⁻¹ or 30-40 m.s⁻¹ by 2050 on average in a region of interest, using the Lines of Evidence Table to assign a likelihood measure (i.e., probability of occurrence) for the projections.

The SMPL is designed to enable a likelihood measure (i.e., probability of occurrence) to be assigned to projections based on considering a comprehensive range of information. This can be done for different projected values (or ranges) within the full distribution of plausible change, noting that the total sum of the percent likelihood measures should equal 100%. The number of different projection ranges selected can be varied depending on the specific application intended, noting that it will always include at least two ranges (e.g., a projected increase in temperature with a likelihood estimate of 99% also implies a 1% likelihood estimate of little change or decrease).

For Step 2, to determine the Projections Likelihood Information for each quantity of interest, model output is considered together with the other information provided in the Lines of Evidence Table (i.e., the observations and physical process understanding). The Lines of Evidence Table can help guide the expert judgement that may be required to produce projections of future change. For example, this could include a greater reliance on direct model output for variables such as extreme temperature for which there is typically higher confidence than for variables such as extreme wind gusts for which a greater reliance on physical process

understanding and other lines of evidence may be practical (e.g., statistical diagnostic methods calibrated to observations data, rather than the use of direct model output).

These steps comprising the SMPL can be applied for a particular time period and emissions scenario(s) of interest, which can help understand the strengths and limitations of projections information for specific variables and regions. For this project, the method is applied for the projected change in climate from the time period 1986–2005 (i.e., a commonly used historical reference period for CMIP5 data (CSIRO & BoM 2015)) to the time period 2040–2059 (i.e., a time period centred on 2050 as requested by energy sector stakeholders).

The RCP8.5 scenario, representing a high emissions pathway for anthropogenic greenhouse gases, is used for the future projections for a number of reasons. Of the set of modelled greenhouse gas emission pathways provided in CMIP5 (which start to deviate from each other after 2005), observed climate change trends for temperature indicate that high emissions pathways (e.g., RCP8.5) have generally been followed more closely than low emissions pathways (e.g., RCP2.6) (IPCC 2013; Schwalm et al. 2020). Additionally, although there is potential for reductions in greenhouse gas emissions and the associated rate of temperature increase later this century, RCP8.5 is used here for the application of this method given that it takes many years after changes in emissions for an emergent change in a climate trend, with the focus for this application on conditions from now until around the middle of this century. However, for applications in which projections are needed based on lower emissions pathways than RCP8.5, methods could be used for scaling the projected changes in extremes according to the global warming magnitude for a particular time period or emissions pathway, such as has been recently demonstrated (NESP 2020). For further details on the relevance of using CMIP5 data for RCP8.5 for projections towards the middle of this century see Schwalm et al. (2020).

For the method application in this study, the information collected in Step 1 for the Lines of Evidence Table is intended to be of relevance for the National Energy Market (NEM) region around parts of southern and eastern Australia including listing any regional variations that might be important to consider within that region.

Table 2.1: Confidence can be assessed based on the degree of evidence and agreement, consistent with IPCC guidelines. The degree of confidence can then be used together with the projections data to help provide likelihood estimates (i.e., probability of occurrence) consistent with Mastrandrea et al. (2011).

	Limited evidence	Medium evidence	Robust evidence
High agreement	Medium confidence	Medium-High confidence	High confidence
Medium agreement	Low-Medium confidence	Medium confidence	Medium-High confidence
Low agreement	Low confidence	Low-Medium confidence	Medium confidence

2.2 Examples of how the SMPL results are being used

The results from applying the SMPL, including the probabilistic projections for extremes and confidence assessment (based on synthesising a comprehensive range of evidence), are being used through the ESCI project in several ways such as listed below. The

nationally consistent calibrated projections presented here are also intended to be of use for a broad range of future applications in many other sectors. This includes for applications such as improved planning and helping to build resilience in relation to the influence of anthropogenic climate change on future hazards in Australia.

- *Enhanced resilience*: Randomised failures are currently used as synthetic input to energy sector modelling for matching supply and demand, including for assessing future changes in the resilience of the NEM. As suggested by energy sector groups, the outputs of the SMPL can be used to refine these failure rates, to help design and plan for a network that is more resilient to future climate change based on considering a comprehensive range of evidence.
- *Enhanced reliability*: The SMPL outputs can be used for providing guidance to accompany the projections data provided as input for the NEM reliability modelling, including insight on whether some datasets might be preferentially weighted over others for some variables/regions.
- *Enhanced design and planning*: Probabilistic projections information for extremes from the SMPL outputs can help understand the future risk of failure for various types of infrastructure, providing important knowledge for the design and planning of individual components in the NEM and other energy sector applications in Australia. Another example includes the use of the 10-yr ARI maps for temperature in AEMO's 2020 Integrated System Plan (ISP).
- *Enhanced guidance for stakeholders on climate risk and hazard scenarios including compound events*: The comprehensive review and synthesis framework of the SMPL is being used to help examine some details for compound event scenarios (i.e., aspects of the combined sets of conditions defined in ESCI project case study activities), intended for use in subsequent risk assessment applications and 'stress testing' activities on climate hazards.
- *Broader applicability*: Although the ESCI project is primarily intended to meet the needs of the electricity sector in Australia, these SMPL results are also intended to have broader benefits including for other sectors, given the relevance of extreme temperatures, winds and bushfire conditions to other sectors.

3. Method application: extreme temperature

3.1 Introduction

The SMPL is applied here for extreme values of daily maximum temperature at a height of 2 m during summer, with a focus on the 10-yr ARI values in south-eastern and eastern Australia. The application of this method follows the steps described in Section 2.

For Step 1 of the method, short summaries are presented below for different aspects relating to future changes in extreme temperature during summer. Regional variations are noted in these summaries if relevant within the region of focus. The summaries are then used to populate the Lines of Evidence Table for extreme temperature (Table 3.1), with key details from the summaries noted succinctly in the table in terms of the degree of influence that this aspect has on extreme temperature and its implied direction of projected change (either an increase, decrease, little change or increased uncertainty).

For Step 2 of the method, the results from the Lines of Evidence Table are used for guidance in producing the Projections Likelihood Information. For this study, this includes the best estimate of the most probable projected change in extreme temperature (presented here as maps) as well as estimates of the 10th and 90th percentile range of plausible change as a measure for indicating the degree of confidence in the future projections. The RCP8.5 emissions pathway from CMIP5 is considered relevant for use here in providing projections towards the middle of this century, given that some key observations for climate are closely tracking that pathway (Schwalm et al. 2020) and noting the considerable time delay from a change in emissions until when an emergent climate response can be detected (including for the extremes considered here). Projections for this pathway are analysed using a historical reference period of 1986-2005 similar to that for the IPCC Fifth Assessment Report using CMIP5 data, with the focus of results presented here on projections centred on 2050 (i.e., for the period 2040-2059).

3.2 Summaries for physical processes (not listed in order of importance)

Soil moisture

Through its control on the exchange of water and energy between the land and the atmosphere, near-surface soil moisture plays a key role in determining air temperature. For example, drier soils can increase the likelihood of extreme temperatures including as has been documented for eastern Australia (Perkins et al., 2015; Herold et al., 2016) and northern Australia (Hirsch et al. 2019). Soil moisture also plays an important role in developing and maintaining extreme heat as documented for Australian heatwaves (Perkins et al., 2016; Wehrli et al., 2019).

On a daily timescale, soil moisture is highly variable in time and space and depends on a range of factors such as recent rainfall, vegetation water use and evaporation (Jovanovic et al. 2008; Ukkola et al. 2019). Soil moisture also varies seasonally and can depend on the previous season's weather conditions and climate states such as large-scale modes of atmospheric and oceanic variability (e.g., ENSO) and associated weather variations as well as longer-term drought conditions. The high level of natural variability of soil moisture in both time and space, as well as the broad range of factors that can influence soil moisture, makes it challenging to determine future changes in these quantities based on model simulations.

In the coming decades, soil moisture is projected to decrease on average over much of Australia, particularly in the southeast where mean rainfall is expected to decrease (particularly during the cooler months of the year) and atmospheric evaporative demand is expected to increase (Berg et al., 2017, CSIRO & BOM 2015). For southern and eastern Australia, more

frequent periods of dry soil are projected to occur in the future with a reasonably high degree of confidence, mostly in winter and spring but also summer (CSIRO & BoM 2015; Ukkola et al. 2020), with this higher frequency of drier soils expected due to higher rates of atmospheric evaporative demand and increased periods of drought. There is potential for increased rainfall during summer, including extreme rainfall in some of the more northeast regions, which could influence soil moisture, with medium confidence (CSIRO & BoM 2015). These previous findings are broadly consistent with new projections of soil moisture produced through the ESCI project (as detailed in a case study report on hydrological applications available from the ESCI website). The level consistency between different studies and modelling approaches can help provide some confidence in the projected future changes of soil moisture.

There are considerable uncertainties around climate models simulations of how soil moisture can influence temperature through land-atmosphere coupling processes. For example, a recent study has shown that climate models may overestimate the coupling between soil moisture and extreme temperatures in wet areas of the globe, so potentially overestimate this aspect to some degree relating to increases in extreme temperatures (Ukkola et al., 2018). There are also uncertainties in the influence of climate change on the direction and magnitude of soil moisture change, including relating to uncertainties in changes to rainfall, potential evaporation and the use of soil water by vegetation under increasing levels of CO₂ (Jovanovic et al. 2008; Ukkola et al. 2020).

In summary, soil moisture can be an important influence on temperature extremes, while noting some uncertainties in the ability of climate models to simulate some processes that are relevant for soil moisture. Projections indicate more frequent periods of dry soil moisture on average in the future during summer in southern and eastern Australia, which will act to increase the risk of extreme temperatures, with medium confidence.

Cloud cover and solar radiation

Extremely high surface temperatures require strong solar radiation (e.g., downwelling shortwave radiation near the surface) which can occur during periods of reduced cloud cover. Conversely, cloud cover can reduce the chance of extreme temperatures. For example, in California, coastal low clouds have been found to moderate heatwaves, particularly the likelihood of a heatwave to extend to the coast (Clemesha et al. 2018).

Projections based on global climate models (GCMs) indicate little change or a small increase in solar radiation in the southeast and east of Australia during summer (CSIRO & BoM 2015). However, the presence of clouds is a major area of uncertainty in climate models, both in terms of future projections and the interaction between clouds and other variables like temperature and atmospheric circulation (Grise & Polvani 2014; Myers & Norris 2015; Voigt et al. 2020). Additionally, there is a large degree of natural variability in cloud cover and solar radiation, which makes it challenging to determine future changes in these quantities based on model simulations.

In summary, cloud cover and solar radiation are important influences on the occurrence of extreme temperature. Future changes for the southeast and central east regions during summer indicate little change or a small increase, with low confidence due to high natural variability and the limitations of climate models in being able to accurately simulate clouds. Regional climate models (RCMs) may provide improvements over GCMs in relation to this aspect, although evidence in the literature is sparse.

Subtropical ridge

An intense subtropical ridge (STR) of mean sea-level pressure is associated with an increase in the mean maximum temperature and the frequency of days above the 90th percentile in southern Australia in all seasons (Pepler et al. 2018). This relationship is strongest in winter and spring, including in southern regions such as Victoria and Tasmania. During summer an intense STR is associated with more hot days in Tasmania but fewer hot days on the east coast including Brisbane. Observations and reanalysis data show the STR has grown more intense in recent decades, which has contributed to observed declines in southeast Australian rainfall (Timbal & Drosdowsky, 2013). It is unknown whether the intensification of the STR has also contributed to past changes in maximum temperature or hot days, but it has contributed to some changes in cold nights in southeast Australia (Pepler et al. 2018).

The STR seasonal cycle is relatively well simulated in CMIP5 and is projected, with high confidence, to intensify in the future (CSIRO & BoM, 2015). In this regard, CMIP5 models represent a significant improvement over CMIP3 models. Despite confidence in the projection of STR intensification, it is uncertain how future intensification will impact future extreme temperatures in Australia. Although CMIP5 models have limited ability to replicate the STR influence on Australian rainfall (CSIRO & BoM, 2015), the STR relationships with temperature are mostly independent of the STR-rainfall relationships (Pepler et al. 2018) and it is a current knowledge gap in the literature as to how well the CMIP5 models replicate the STR relationship with extreme temperatures.

In the Southern Hemisphere, the STR intensification and other measures of tropical expansion have been linked to climate change (Nguyen et al. 2015; Grise et al. 2019) with some contribution from ozone depletion in the summer months as well as natural variability (Garfinkel et al., 2015; Waugh et al., 2015). Climate models consistently project a future southward shift and intensification of the subtropical ridge (Kent et al. 2013; Grose et al. 2015). However, this may be masked by the influence of ozone hole recovery during the summer months in coming decades to some degree (IPCC 2013).

In summary, the STR has historically had a significant influence on the occurrence of extreme temperatures, with more intense STR associated with hotter summer temperatures particularly in southern Australia. Although CMIP5 models do a reasonable job of simulating the STR, including an increase in intensity being likely in the future, the impact of the STR on future extreme temperatures is somewhat uncertain. As STR is a large-scale feature with links to broader-scale processes such as tropical expansion, RCMs may offer relatively limited improvement over GCMs in representing the STR. However, RCMs may be better able to simulate the impacts of the STR on local climate extremes, due to better simulation of interactions between the large scale and local factors such as cloud cover.

Cold Fronts

Frontal systems are major drivers of extreme temperature events in southern Australia. Strong northwesterly winds prior to cold fronts enhance the advection of extreme heat from inland Australia towards the southeast regions during summer. Some studies suggest relatively little change in the frequency of fronts in southeast Australia and a slight decrease in their mean intensity over recent decades (Rudeva & Simmonds, 2015), while some studies also indicate the frequency of fronts has decreased in some regions of southeast Australia such as for the eastern seaboard (Pepler et al. 2021).

Climate models are generally able to simulate the average annual frequency of fronts in the Australian region during winter, but relatively few studies have examined this during summer (Catto et al. 2015; Blázquez & Solman 2017). Climate model projections have a weak increase in the frequency and intensity of all fronts in southern Australia, but the available

projections do not distinguish the cold fronts associated with northwesterly winds from weaker warm and stationary fronts (Catto et al. 2014; Blázquez & Solman 2019). Using the older CMIP3 climate models, a simple temperature-based proxy for very extreme cold fronts associated with summer temperature extremes and bushfires indicated a likely future increase in the frequency of frontal systems (under both medium and high emissions scenarios), increasing from ~0.5 events per year in the current climate to 1-2 events per year by the end of the 21st century (Hasson et al. 2009). Considering studies such as these, considerable uncertainties remain in relation to extreme temperature events associated with fronts in the during summer and how these events could potentially change in the future, including considerable uncertainties in relation to future changes in the influence of fronts on the occurrence frequency of extreme temperatures in southern and eastern Australia.

In summary, observations indicate frontal activity has undergone little change in southern and eastern Australia during summer, with considerable uncertainty for future projected changes in frontal systems and their impact on extreme temperatures. Given that fronts are synoptic-scale systems which GCMs can simulate reasonably well, there may not be a large benefit from using RCMs to examine future frontal system activity compared to other factors like clouds and solar radiation. However, RCMs could potentially provide value for some aspects relating to fronts such as their interaction with terrain and associated extreme weather impacts for localised regions in some cases.

Blocking / high pressure systems

For southeast Australia, anticyclones (high pressure systems) are typically associated with cool southerly winds to the east of the high-pressure system and warm northerly winds to the west. A persistent and slow-moving ('quasi-stationary') high pressure system in the Tasman Sea is often referred to as a blocking high and can cause extreme heat in southeast Australia (Marshall et al. 2013; Boschat et al. 2015; Gibson et al. 2017). This is somewhat distinct from so-called "split-flow" blocking typically to the south of Australia, that can sometimes cause cooler temperatures in some parts of southern Australia with climate models generally simulating a decrease in the frequency of winter split-flow blocking in the Tasman Sea but little change during the summer months (Patterson et al. 2019) (also noting the focus of this study on summer rather than winter).

GCMs are generally able to simulate anticyclones, as they tend to be large-scale systems, but may underestimate their persistence and the frequency of long periods of 'quasi-stationary' blocking (Woollings et al. 2018). GCMs are able to simulate some of the larger-scale pressure patterns associated with heatwaves in southeast Australia, including anomalously high pressure in the Tasman Sea. Anticyclones tend to be stronger and slightly further south in CMIP5 projections of future climate, which could contribute to increased temperature extremes in the future (Purich et al. 2014). The mean sea level pressure over the Tasman Sea is also projected to increase in the 21st century in CMIP5 models (Hope et al. 2015).

In summary, blocking / high pressure systems, particular in the Tasman Sea region, can influence the occurrence of extreme heat events in southeast Australia during summer. Although there is some potential for this to increase in the future there are considerable uncertainties around this based on existing studies. GCMs can provide a reasonable representation of some of the larger-scale pressure features relevant to the advection of hot air from further inland over the continent, while noting some blocking events can be better represented by finer resolution models (Dawson et al. 2012).

Tropical cyclones

The occurrence of tropical cyclones (TCs) in northern Australia has been linked with the intensification of heat extremes in southern Australia, including in southeast Australia during summer (Parker et al. 2013; Quinting & Reeder 2017; Quinting et al. 2018). For example, the extreme heat experienced around the time of the Black Saturday fires in 2009, which set new temperature records for daily maximum air temperature for Melbourne and surrounding locations, was associated with the presence of a TC (Parker et al., 2013). Observations indicate a decrease in occurrence frequency of TCs for the Australian region over recent decades (Dowdy 2014; Chand et al. 2019).

Future projections of TCs during summer for the Australian region indicate a small decrease in their frequency (medium confidence) (Bell et al. 2019). However, the frequency of intense category 4 and 5 TCs may not change or increase slightly, along with some poleward migration (low confidence) (CSIRO & BoM 2015; Knutson et al. 2020; NESP 2020). In general, GCMs have insufficient spatial and temporal resolution to adequately simulate tropical cyclones. RCMs generally have finer resolution and better resolve tropical cyclones, although RCMs still do not fully capture all relevant processes. For this reason, additional methods for cyclone projections can also be useful to consider, such as synthetic cyclone tracks, in addition to dynamic modelling. For further details on TCs in a changing climate see NESP (2020).

Modes of variability - ENSO

The relationship between the El Niño-Southern Oscillation (ENSO) and temperature extremes is complex. Across most of northern and eastern Australia, the frequency, duration and amplitude of heatwaves increases during El Niño years (Perkins et al. 2015; Loughran et al. 2019). However, in parts of the southeast including Victoria, there is either little relationship between ENSO and heatwaves or an increase during La Niña years, related to an increase in tropical convection and more slower-moving weather systems (Parker et al. 2014; Perkins et al. 2015). El Niño years are also associated with reduced cloud cover leading to higher temperatures and an increase in the temperature of the hottest day of the year across most of Australia (Arblaster & Alexander, 2012).

Although correlations between mean temperature and ENSO conditions have been examined in numerous previous studies (such as some discussed in this section), this has not been examined in much detail for more extreme measures of temperature. To help address that knowledge gap, correlations are presented in Figure 3.1 for ENSO, as well as for SAM and IOD (relating to subsequent sections below). The general patterns of correlation (indicating the strength of the relationship with ENSO) are broadly consistent for mean and extreme temperatures, indicative of higher temperatures in general occurring for El Niño than La Niña conditions.

There are considerable uncertainties around how ENSO conditions (including extreme ENSO events) may change later this century based on GCMs (CSIRO & BoM 2015). Projections of an increase in frequency of ENSO events being sensitive to the model used (Freund et al 2020) and frequency of extreme ENSO events sensitive to the definition used (Marjani et al. 2019). As the teleconnections between ENSO and Australian rainfall and temperatures have varied over time (Power et al. 1999), the strength of these relationships may also change in the future (Fasullo et al. 2018). However, some studies have suggested there might be an increase in the number of strong El Niño and La Niña events in future (Cai et al. 2018a). As modes of variability such as ENSO are phenomena generated in association with very large-scale atmosphere-ocean interactions, RCMs do not provide benefits over GCMs in simulation how the modes of variability may change in the future. However, RCMs may provide further detail on how modes of variability influence local and regional climate,

including cloud cover. In fact, RCMs have been shown to capture the historical teleconnection between ENSO and Australian maximum temperatures quite well (Fita et al. 2016).

In summary, the influence of ENSO on future extreme temperature events involves considerable uncertainties. The uncertainties in ENSO simulation are not able to be resolved through the use of currently available RCM data (e.g., no coupled RCM simulation has been performed to date over a domain large enough to encompass the processes leading to ENSO) but RCMs may help in simulating local responses to large-scale drivers such as ENSO.

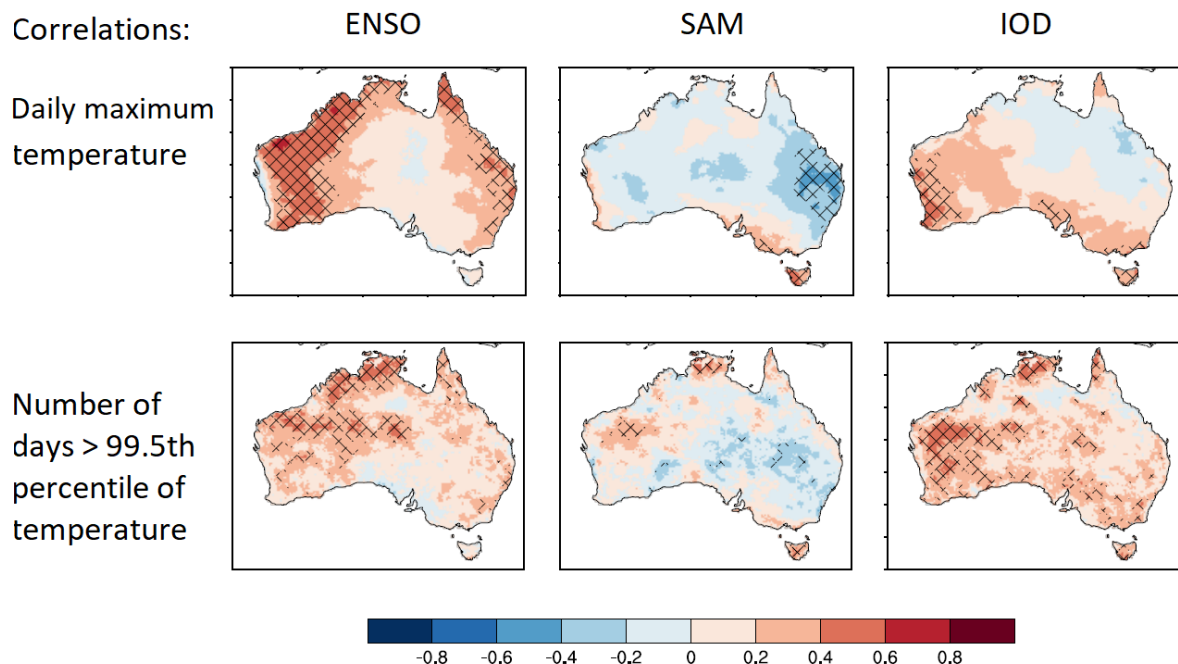


Figure 3.1: Correlations between temperature and climate measures. This is presented in the upper row of panels for daily maximum temperature (using average summer values for the months December to February: DJF) and measures representing different modes of variability including ENSO (using the NINO3.4 index), SAM (using the SAM index) and IOD (using the DMI index). Similar correlations are also shown in the lower row of panels, but for the number of days with temperature above the 99.5th percentile during summer. These correlations are all based on the period from 1979 to 2019, using one value for each summer period (DJF). NINO3.4 and DMI data are attained from the NASA ESRL (https://psl.noaa.gov/gcos_wgsp/Timeseries/) while SAM data are from <https://legacy.bas.ac.uk/met/gjma/sam.html>. Pearson's correlation coefficient, r , is shown with stippling corresponding to statistically significant values at the 95% confidence level (2-tailed).

Modes of variability – IOD

The IOD mostly influences Australian weather during the winter and spring, so it has little relationship with extreme heat during the summer months in general (Perkins et al. 2015), as well as noting interactions between the Indian Ocean Dipole (IOD) and ENSO (Cai et al. 2019). The relationship between IOD and average values of daily maximum temperature is broadly similar to that for the more extreme values of daily maximum temperature, with positive correlations through southern and eastern Australia in general (Fig. 3.1). There is some indication that extreme positive IOD events may become more frequent in the future (Cai et al.

2018b) but there is considerable uncertainty in the ability of climate models to simulate such events (CSIRO & BoM 2015).

Modes of variability - SAM

The Southern Annular Mode (SAM) is a large-scale alternation of atmospheric mass between the middle and high latitudes. The positive phase is associated with a higher-than-normal mean sea level pressure in middle latitudes and lower pressure in high latitudes. During a positive phase of the SAM there is a southward shift for the belt of westerly winds that circles Antarctica, while the opposite occurs during the negative phase. The La Niña phase of ENSO increases global mean temperature and can contribute to a negative shift in the SAM (Wang & Cai 2013).

Positive SAM is associated with a decreased likelihood of extreme heat during the spring, but correlations are more mixed during the summer months (Hendon et al. 2007; Marshall et al. 2013; Perkins et al. 2015). The relationship between SAM and average values of daily maximum temperature is broadly similar in spatial patterns (e.g., sign of correlation, from Figure 3.1) to the case for the relationship between SAM and the occurrence of more extreme values of daily maximum temperature, with generally weak correlations or a negative correlation in central eastern regions (particularly for mean temperature). A strong negative SAM is also associated with sudden stratospheric warmings (as occurred in the 2019 Austral spring), which can cause extreme heat during spring and early summer (Lim et al. 2019), potentially associated with some of the negative correlations apparent in Figure 3.1 for the central east region.

SAM has been becoming more positive in recent decades, particularly during the summer months (Marshall, 2003), which has been linked to a combination of increased greenhouse gases as well as ozone depletion and natural variability (Garfinkel et al. 2015; Waugh et al. 2015). CMIP5 models project a robust shift towards more positive values of SAM in all seasons during the 21st century (Lim et al. 2016), although this may be masked to some degree by the influence of ozone hole recovery during the summer months in coming decades (Banerjee et al. 2020). In summary, climate models can simulate SAM well, but projections of a positive trend in SAM would likely cause little change in the risk of heat extremes during summer apart from potentially central east (noting a negative correlation with temperature as well as links with sudden stratospheric warmings (Lim et al. 2019) for which future projected changes are not currently known).

Modes of variability – MJO

The Madden-Julian Oscillation (MJO) is the dominant mode of atmospheric intra-seasonal variability and the cornerstone for sub-seasonal prediction of extreme weather events (Wang et al. 2019). Extreme heat in south-eastern Australia is more common during MJO phases 2 and 3 in spring and phases 3-6 in summer (Marshall et al. 2013; Parker et al. 2014). The influence of climate change on the MJO is uncertain, with less confidence in changes in MJO-related wind and circulation anomalies than for rainfall (Maloney et al. 2019), noting that CMIP5 GCMs are not able to provide a good representation of the MJO (CSIRO & BoM 2015). Consequently, this remains an uncertain factor in relation to extreme summer heat in the future including for southern and eastern Australia.

Urban effects including urban heat island

The temperatures in urban environments are typically warmer than the surrounding rural areas, particularly at night. This is a consequence of changes to many surface properties

which alter the surface energy budget, in addition to the presence of additional sources of anthropogenic heat. The additional overnight heat can contribute to enhanced heat stress on urban populations, although this may be partially counteracted by lower humidity (Fischer et al. 2012; Williams et al. 2012). While some studies have suggested that the urban heat island (UHI) is more intense during hotter conditions, this varies between studies and between different areas of the world (Scott et al. 2018, Zhao et al. 2018, Chew et al. 2020). Due to the small spatial scale of cities and the complexity of their terrain, these are typically only well simulated in high resolution regional downscaled simulations, not coarse GCMs (Argueso et al. 2015; Wouters et al. 2017).

The UHI effect adds a few degrees to temperatures over urban environments (Gartland 2011). This has been shown over the largest cities in Australia including Sydney (Argueso et al. 2014), Melbourne (Imran et al. 2019), Brisbane (Chapman et al. 2019) and Adelaide (Guan et al. 2016). The UHI has been found to exacerbate temperature extremes at night during heatwaves in these cities (Argueso et al. 2015; Imran et al. 2019; Rogers et al. 2019). Daytime maximum temperatures during heatwaves reflect the standard UHI addition to the temperature of the surrounding areas. The increased night-time temperatures mean that systems have less opportunity to cool overnight which poses a hazard for some systems including human health.

Cities will likely experience similar temperature increases due to global warming as their surrounding regions but will remain warmer due to the UHI. It is uncertain whether the intensity of the UHI will change as the planet warms, with any changes sensitive to changes in other factors such as green space (i.e., vegetated areas including tree cover), soil moisture and circulation (Fischer et al. 2012; Zhao et al. 2018). However, in regions which are currently on the urban fringe, future population growth and urban expansion is expected to result in additional increases in hot extremes beyond that expected from climate change alone (Argueso et al. 2015; Wouters et al. 2017). In summary, the UHI effect means that extreme heat events are more severe in urban regions, regardless of climate change, and urban areas are often not well simulated in coarse resolution GCMs, although this can be better resolved in RCMs with dedicated urban parameterisations. It is unclear if this effect will change in the future, but future warming is expected to be larger in areas which are also experiencing urbanisation.

3.3 Summaries for historical information

Observed trends

Extreme temperature events have been steadily increasing in frequency and intensity throughout Australia due to increases in atmospheric concentrations of greenhouse gases (CSIRO & BoM 2015; BoM & CSIRO 2020). For example, the number of extreme heat records in Australia has outnumbered extreme cool records by about 3 to 1 since 2001 for daily maximum temperatures (BoM & CSIRO 2020), characteristic of a shift in the full distribution of temperature values due to anthropogenic global warming. In parts of southeast Australia, the hottest summer days have increased by a larger degree than expected from the change in mean temperatures alone (Gross et al. 2019). Heatwave events have also increased in intensity, frequency and duration across Australia in recent decades (Perkins-Kirkpatrick et al. 2016). The 2019 year was Australia's hottest on record, as well as having 42 days when the Australian area-averaged daily mean temperature was above the 99th percentile (which also set a new record for that measure of extreme temperatures for individual days).

Model assessment

The ability of climate models to simulate aspects such as the seasonal cycle, observed trends, spatial detail and extremes is important for helping to understand the degree of

confidence in future projected changes based on these models. Assessments as presented in CSIRO & BoM (2015) indicate that global models provide a reasonably good representation of these aspects, including regional and seasonal temperature variations through Australia as well as the observed trends.

3.4 Summaries for projected changes

Several datasets are available for future projections of values corresponding to 10-year ARI of daily temperature. The datasets include dynamical downscaling using the CCAM modelling approach (conformal cubic atmospheric model) applied to 5 GCMs (ACCESS1-0, CanESM2, GFDL-ESM2M, MIROC5 and NorESM1-M), dynamical downscaling using the BARPA modelling approach (Bureau of Meteorology Atmospheric Regional Projections for Australia) applied to the ACCESS1-0 GCM for eastern Australia, dynamical downscaling using the NARCliM modelling approach (NSW and ACT Regional Climate Model) applied to 3 GCMs (ACCESS1-0, ACCESS1-3 and CanESM2, with 2 configurations of each). These datasets have all been calibrated using the quantile matching for extremes (QME) approach described in Dowdy (2020b). Calibrated data (using QME) were also available based on four GCMs for use in this analysis (for ACCESS1-0, CNRM-CM5, GFDL-ESM2M and MIROC5 GCMs). For further details on the selection and assessment of these models see Thatcher et al. (2021). It is generally recommended to use a broad range of modelling approaches (rather than only relying on a single method) when trying to sample the uncertainty space for plausible future changes, such that a focus on this report is on the combined results from this 16-member ensemble of calibrated projections datasets (i.e., 5 from CCAM, 1 from BARPA, 6 from NARCliM and 4 from GCMs). This is particularly important for helping to provide enhanced confidence in projections of extremes, as is a focus here.

To calculate the values corresponding to the 10-year ARI, a Generalised Extreme Value (GEV) approach was used. This is based on 20-year time slices: using 1986-2005 for the historic period and 2040-2059 for the future climate projection for the RCP8.5 emission pathway (noting that these projections data are also available for other time periods throughout this century and historical periods, as well as for RCP4.5). The projections from these different methods are presented in Figure 3.2 for the GCMs, CCAM, BARPA and NARCliM ensembles, all with QME calibration applied. Each method shows clear increases in extreme temperatures projected for the future climate. Further details on these various different datasets and methods are available in Thatcher et al. (2021).

In addition to these results based on CMIP5, some results have recently been published based on some CMIP6 projections (Grose et al. 2020). Those results show broadly similar changes for temperature extremes in Australia to those based on CMIP5 projections, noting that subsequent studies will continue to examine this further including based on a larger set of CMIP6 models than was available for that study.

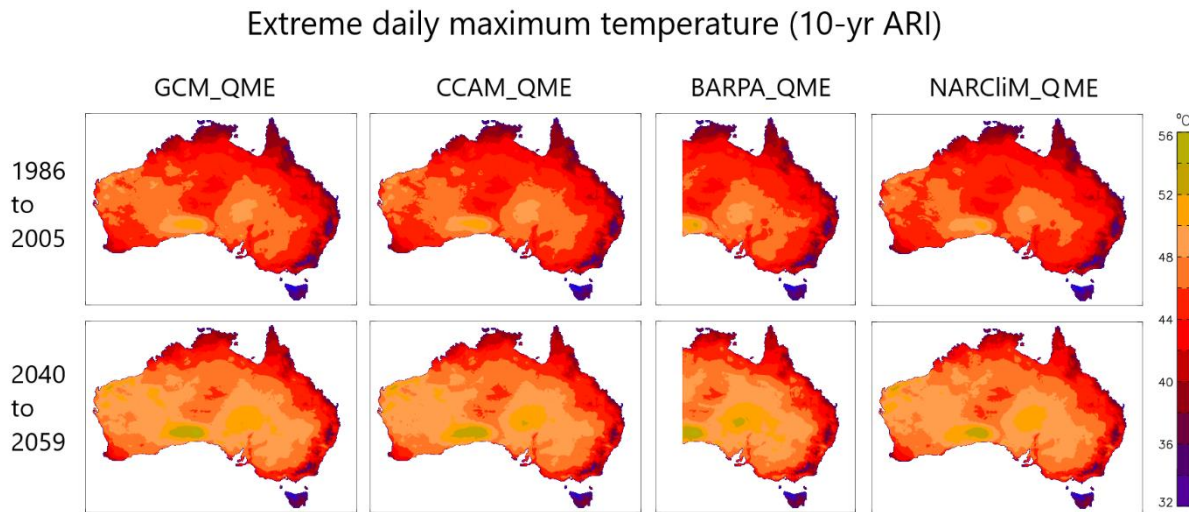


Figure 3.2: Projected change in values corresponding to the 10-year ARI for daily maximum temperature at a height of 2 m. This is shown based on GCMs (left panels), CCAM (second to left panels), BARPA (second to right panels) and NARClM (right panels), all calibrated using the QME method. Maps are shown for Australia based on the model ensemble average in each case. This is presented for the historical climate based on 1986-2005 (upper panels) and future simulated climate based on 2040-2059 under a high emissions pathway RCP8.5 from CMIP5 (lower panels).

3.5 Lines of Evidence Table

Table 3.1: Lines of Evidence Table for extreme daily maximum temperature at a height of 2 m, with a focus on summer in the southeast and east of Australia. The degree of influence is listed in black, followed by whether this information implies an increase (red), decrease (blue) or little change (black) in extreme temperature, as well as by increased uncertainty (purple) in the direction of change. The rows of information are not in order of importance.

Physical processes	
Soil moisture	Moderate influence. More frequent dry soil with medium confidence; potential increase in northeast. Influence on temperature potentially overestimated. Regional models likely to add value.
Cloud cover and solar radiation	Moderate influence. Low confidence in little change or a small increase. Regional models likely to add value.
STR	Large influence, primarily in southern Australia. Potential increase with low confidence in future influence on extreme temperature.
Fronts	Moderate influence. Future change uncertain.
Blocking	Moderate influence. Future change uncertain.
Tropical cyclones	Small influence. Fewer in the future (medium confidence) from global models; regional models likely to add value.
ENSO	Small to moderate influence. Uncertain future change; potentially more frequent strong El Niño events (low-medium confidence).
IOD	Small to moderate influence. Uncertain future change; potentially more frequent strong IOD events (low-medium confidence).
SAM	Small to moderate influence. Positive trend in SAM relevant for northeast region temperatures (medium confidence).
MJO	Small influence. Uncertain future change.

Urban effects	Important for local heat extremes. Urban heat island adds a few degrees and stays reasonably consistent in future (high confidence); increased temperature extremes in areas of future urban growth.
Assessment for historical period	
Seasonal cycle	Models reproduce the seasonal cycle and spatial variability (high confidence).
Historical trend	Strong increase from observations (high confidence). Models reproduce the trend well (high confidence).
Projected future change	
GCMs (CMIP5 and CMIP6)	Strong increase (high confidence).
CCAM	Strong increase (high confidence).
NARCliM	Strong increase (high confidence).
BARPA	Strong increase (high confidence). Based on one model to date.
Very fine resolution	Uncertain future change due to lack of available data and analysis.

3.6 Projections Likelihood Information

The Lines of Evidence Table (Table 3.1) shows considerable agreement on increased extreme temperatures in a warming climate, including 10-year ARI daily maximum temperatures in the southeast and east of Australia during summer as is a key focus here. Although there are some physical processes noted that add uncertainties, particularly based on GCM projections data, the RCM approaches (CCAM, BARPA and NARCliM) can help with the simulation of some of these processes. Therefore, the relatively high level of agreement between RCM approaches helps add some confidence for projected future increases. Based on this overall assessment considering this wide range of factors, there is *Very High Confidence* in the projected direction of change, with a future increase in 10-year ARI temperatures being *Very Likely* (i.e., 90-100% probability).

Based on the above points and details in the Lines of Evidence Table, projected changes for 10-year ARI temperatures for the 2050 climate are considered here based on the 16-member ensemble of calibrated projections datasets, combined based on equally weighting each member of this ensemble. The ensemble median is used as a central estimate of the most probable projected change (Figure 3.3). As an estimate of the range of plausible values from the 16 ensemble members, the second lowest value from the ensemble is used for the 10th percentile and the second highest value from the ensemble is used for the 90th percentile. These values are calculated individually at each grid cell location for the median and percentile estimates.

The results show that the future projected temperatures are higher than for the historical period, including for the lower estimate corresponding to the 10th percentile of the model ensemble in the future, as well as for the median and upper estimate (90th percentile). This highlights the considerable degree of agreement between these diverse modelling approaches.

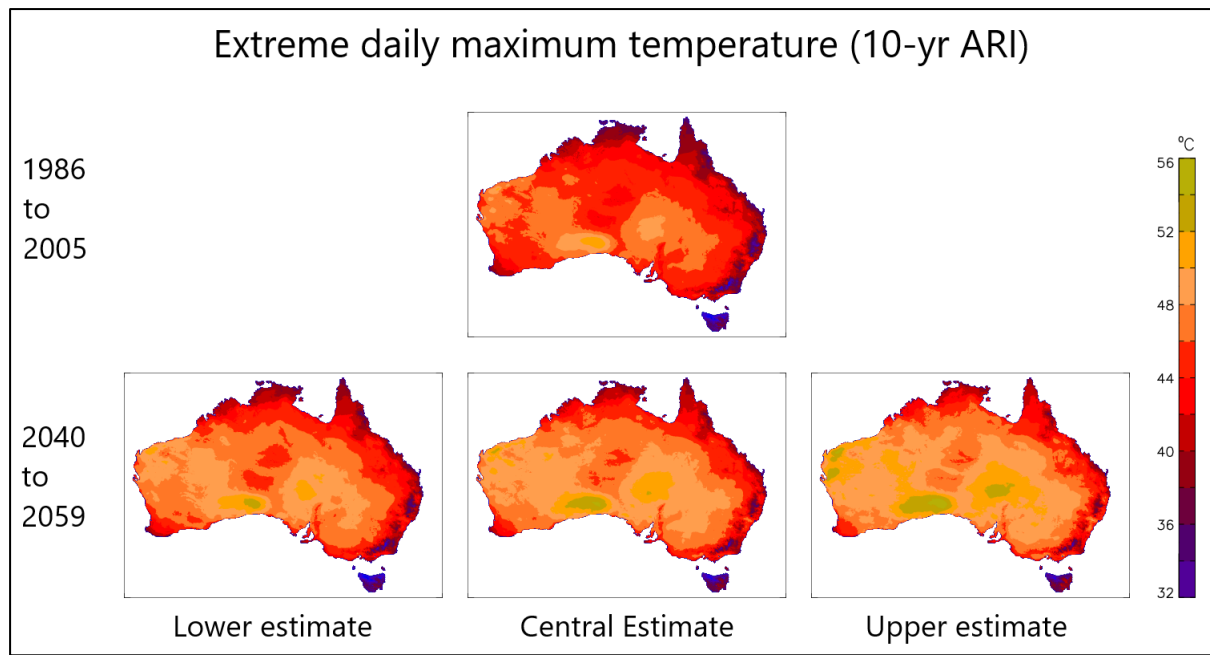


Figure 3.3: Projected values corresponding to the 10-year ARI for daily maximum temperature at a height of 2 m, based on a 16-member ensemble of calibrated model projections. Maps are shown through Australia for the historical period (based on 1986-2005; upper panel), as well as for the future simulated climate (based on 2040-2059 under a high emissions pathway RCP8.5: lower panels) including a central estimate with lower and upper estimates also provided.

4. Method application: extreme winds

4.1 Introduction

The SMPL is applied in this section similar to in Section 3, but with a focus here on extreme winds during summer (December–February) in the southeast and east of Australia. Destructive winds in Australia can be caused by severe thunderstorms (i.e., localised weather systems characterised by strong and deep moist convection) or by larger-scale synoptic systems such as tropical cyclones or extratropical cyclones and their associated frontal systems. In addition, systems on these two different scales can occur simultaneously in the same geographic region, resulting in compound events with enhanced impacts (Dowdy & Catto 2017).

Convective hazards including damaging wind gusts from severe thunderstorms occur most frequently during the warmer months of the year (Brown & Dowdy 2021). The impacts of tropical cyclones (TCs) and a type of midlatitude cyclone known as east coast lows (ECLs) are mostly confined to some near-coastal regions of eastern Australia (e.g., Dowdy et al. 2019a). Further details are available on climate change influences on ECLs and TCs in a changing climate (Chand et al. 2019; Dowdy et al. 2019a; NESP 2020). In contrast, convective systems (severe thunderstorms) affect all of Australia and have been responsible for most of the surface wind gusts which exceed the 10-year ARI near the major population centres including in the southeast and east of Australia (Holmes 2002), such that the SMPL is applied here with a focus on severe convective wind gusts. Other phenomena including TCs and ECLs are also considered here in some sections for completeness.

For Australia, wind gusts are defined by a 3-second average wind speed. Severe convective wind gusts (SCWs) are considered for the purposes of this study as exceeding 25 m.s^{-1} , at a height of 10 meters above ground level, caused by thunderstorm outflow. This threshold (equivalent to exceeding 90 km.hr^{-1}) is consistent with the threshold used for severe weather forecasting and operational warnings produced by the Australian Bureau of Meteorology. While gusts of around 25 m.s^{-1} may not always be destructive, it is noted that this definition is based on exceeding that value and therefore also includes higher wind speeds (e.g., around 45 m.s^{-1}) which have a higher chance of causing property damage. This covers a range of ARI values consistent with wind speeds such as provided in current Australian standards, including spanning a range broadly similar to the values for the 10-yr ARI in southern and eastern Australia assuming flat, open terrain (Holmes, 2002). The atmospheric environments which produce this range of wind gusts (roughly around $25\text{--}45 \text{ m.s}^{-1}$) are typically characterised by unstable atmospheric conditions (i.e., conducive for convection) as well as likely to include conditions favourable for convective organisation which can lead to increased severity of hazards (such as can be associated with strong wind shear between vertical levels (Taszarek et al. 2017)). Tornadoes are a special class of severe convective winds that are not considered here, including due to their very rare occurrence at a given location and their very small spatial scale, as well as noting that the design standards widely used in Australia do not intend structures to withstand the occurrence of a tornado.

4.2 Summaries for physical processes

Thunderstorm environments

Environments conducive for thunderstorm occurrence are often defined by atmospheric instability and moisture availability, while severe thunderstorms may also require other contributing factors such as vertical wind shear (that is when the wind changes in speed and/or direction with height) which can help organise the structure of a severe thunderstorm (Brooks

et al. 2003; Taszarek et al. 2017). Convective instability depends on the vertical profile of temperature and moisture. Globally, the vertical temperature lapse rate (the rate of temperature decrease with height) is predicted to decrease/stabilise (increase/destabilise) into the future in the extratropics (tropics) due to different rates of warming in the lower atmosphere compared to the upper atmosphere (Bony et al. 2006), while atmospheric moisture content is predicted to increase by about 7% per degree of warming based on the Clausius-Clapeyron relation (IPCC 2013). Vertical wind shear is predicted to decrease in the global mid-latitudes due to reduced zonal surface temperature gradients via the thermal wind relation (IPCC 2013; CSIRO & BoM 2015).

Combining these factors through the use of environmental thunderstorm diagnostics applied to model data, the frequency of thunderstorm environments has been projected to increase during the coming century in the United States (Trapp et al. 2007; Diffenbaugh et al. 2013; Gensini et al. 2014; Seeley & Romps 2015) and Europe (Púčik et al. 2017), likely driven by increases in atmospheric moisture content resulting in increases to convective available potential energy. This is similar to results for eastern Australia during the warm season (Allen et al. 2014), noting various model uncertainties remain unquantified for the Australian region (e.g., a need for additional studies on variations in projections between a broader range of models and methods).

Historical increases in the frequency of thunderstorm environments have been indicated by reanalysis data for some near-coastal parts of southeastern Australia, but with decreasing frequency overall for most regions of Australia (Dowdy 2020a), while noting those results were for thunderstorm activity in general rather than for the more severe thunderstorm events that can cause SCWs. Historical increases in thunderstorm environments have been reported for Europe (Rädler et al. 2018), although trends are less certain in North America, which may partially be due to increasing convective inhibition (CIN) offsetting increases in convective instability (Taszarek et al. 2020), a factor which limits thunderstorm development. A recent study indicates CIN projected to increase over most land areas in the future (Chen et al. 2020).

Some regional projections studies in the United States have noted that CIN is likely to increase in a future climate, which could offset increases to available convective energy as discussed above (Hoogewind et al. 2017; Rasmussen et al. 2017). These changes could potentially combine to result in less frequent but more intense thunderstorm initiations, although a modern GCM ensemble has suggested that CIN could decrease on days with high amounts of instability (Diffenbaugh et al. 2013). In addition, CIN tends to be poorly resolved in large-scale dynamical models due to issues in representing fine-scale features of the vertical temperature profile (King & Kennedy 2019), such that future changes in this quantity represent a key uncertainty in thunderstorm projections.

Overall, there is low confidence in an increasing frequency of favourable environments for severe thunderstorms during summer in Australia, including based on results from other regions and the work of Allen et al. (2014) for projections of future changes in Australia (while noting that as based on a relatively limited range of modelling approaches). Significant uncertainties which remain include a lack of projections data for Australia based on a broad range of modelling approaches, as well as the influence of CIN in a changing climate on the potential for severe thunderstorm occurrence. It is noted that favourable environmental factors are necessary, but not sufficient for thunderstorm occurrence (depending on initiating mechanisms) and also that additional factors are required for SCW occurrence.

Severe convective wind environments

In addition to the thunderstorm environmental factors mentioned above, there are additional factors which can be conducive to SCW production, as well as noting different modes of thunderstorm systems that can be associated with severe convective winds (Smith et al. 2012). SCWs can be formed due to intense downdrafts within thunderstorms, with the downdrafts initiated due to the evaporative cooling of precipitation which causes cold, dense air to accelerate downwards, also aided by the weight of the precipitation itself. Downdrafts which reach the surface will transfer their momentum (as well as background momentum from higher up in the atmosphere) into the horizontal, causing severe wind gusts. This process depends on environmental factors including a relatively dry lower atmosphere combined with a steep temperature lapse rate as well as strong environmental wind speeds (Proctor 1989; Kuchera & Parker 2006; Brown & Dowdy 2021), although the relative importance of these may vary with convective mode (Doswell & Evans 2003). It follows that the variability of SCWs on climate timescales may be different to thunderstorms in general (Brooks 2013). The impact of climate change on individual convective hazards, such as severe surface winds, is highly uncertain (Allen 2018). However, recent work in Australia has suggested the potential for increases in the frequency of severe convective wind environments into the late century (Spassiani 2020), which is similar to historical findings for Europe (Rädler et al. 2018). There have also been future projections of severe convective wind speeds for Tasmania (Cechet et al. 2012), applying a severe thunderstorm diagnostic to historical observed wind speeds. New projections of SCW environments are presented in Section 4.4 (with details on this method available in Brown & Dowdy (2021)).

Thunderstorm initiation

Given an environment favourable for severe convection (i.e., thermodynamically unstable conditions), synoptic systems (extratropical cyclones, fronts, jets), atmospheric waves and orographic influences (sea-breezes and mountains) can help provide thunderstorm initiation. Projection studies tend to indicate that changes in synoptic initiation mechanisms such as mid-latitude extratropical cyclones and east coast low systems are not clear for Australia during the summer months (Catto et al. 2014; Pepler et al. 2016; Dowdy et al. 2019a). Cyclone-related convection is sensitive to changes in coastal sea surface temperature gradients (Chambers et al. 2015), noting that the Tasman Sea east of Australia is a region of accelerated ocean warming. Projections related to fronts are discussed in detail within Section 3, which indicates there is a considerable amount of uncertainty, with little or no change being the most plausible outcome.

There is relatively little information on changes to orographic flows such as sea breezes; however, the strength of the sea breeze is strongly related to the land-sea temperature contrast, which is expected to increase into the future. One study found an increase in the frequency and intensity of sea breezes in Adelaide between 1955-2007 (Masouleh et al. 2019). Regional model simulations at 20 km resolution have been shown to provide a reasonable simulation of the sea breeze in the Mediterranean region (Drobinski et al. 2018), although convective parameterisations are less skilful in simulating sea breeze-related CIN (Birch et al. 2015). In summary, changes to thunderstorm initiation mechanisms in Australia during the summer are highly uncertain.

Modes of variability – ENSO, IOD and SAM

Details on modes of variability were provided in Section 3, including in relation to ENSO, IOD and SAM conditions in a changing climate. Building on that information, aspects specifically relating to SCWs are summarised here.

Thunderstorm environments are not significantly related to ENSO conditions in general for Australia, apart from in northern Cape York Peninsula where they are more likely during La Niña than El Niño conditions (Allen & Karoly 2014; Dowdy 2016, 2020a). However, it is still feasible that ENSO may potentially modulate convective initiation mechanisms, such as by reducing cloud cover during El Niño conditions and enhancing the sea-breeze circulation in south-east Queensland which might increase the frequency of severe thunderstorm events (Soderholm et al. 2017) while noting considerable uncertainties around the role of ENSO on such processes. It is likely that there is not a strong relationship between ENSO and synoptic-scale initiation mechanisms, including little or no relationship found between ENSO and fronts in southern Australia or between ENSO and ECLs in eastern Australia (Rudeva & Simmonds; Power and Callaghan 2016; Dowdy et al. 2019a). The relationship between ENSO and SCW environments is shown here in Figure 4.1a, suggesting very little relationship with ENSO in eastern Australia during the summer. In summary, the influence of ENSO on SCWs appears to be relatively weak while noting considerable uncertainties based on limited data and analysis to date, as is also the case for the relationship between ENSO and severe thunderstorm occurrence as well as between ENSO and synoptic initiation mechanisms (including fronts and cyclones in southeast Australia during summer).

The IOD has previously been found to not have a notable influence on thunderstorm activity in Australia during summer including in southern and eastern Australia, as detailed in Dowdy (2020a), while noting that study was not specifically focussed on severe thunderstorms which could potentially have different characteristics to thunderstorms in general. The influence of the IOD on severe thunderstorms in Australia is currently uncertain based on a lack of previous analyses (Allen & Allen 2016), although the IOD may relate to extreme wind gust variability in general, with potential for higher occurrence frequencies during negative IOD phases (Azorin-Molina et al. 2021). The influence of the IOD on SCW environments is not significant during the summer in southern and eastern Australia (Figure 4.1c), broadly similar to the lack of correlation between the IOD and thunderstorm environments (Dowdy 2020a), with some indication of a relationship in northeast regions.

Similar to the IOD and ENSO, the influence of SAM on severe thunderstorms in Australia is largely uncertain. Although no consistent relationship has been found previously with thunderstorm environments (Dowdy 2020a), it is plausible that a positive SAM phase with reduced westerlies in eastern Australia during the summer may enhance moisture availability due to increased onshore flow in some regions, thereby increasing the frequency of favourable thunderstorm environments if such cases were to occur. In a negative SAM phase, the strengthening of background winds and a relatively dry lower atmosphere due to enhanced westerlies plausibly could increase the potential for an environment favourable for strong convective downbursts (albeit through a different mechanism to that described above for the positive SAM phase). Although it is not clear based on considering such physical processes as to which phase of SAM may be more likely to generate SCWs, it appears that the negative phase of SAM is more conducive than the positive phase for SCW environments based on the results in Figure 4.1b. In addition, enhanced westerlies and associated cold fronts during the negative phase of SAM (Rudeva & Simmonds, 2015) may increase the frequency of synoptic initiation mechanisms in some southern regions, and extreme wind gusts from station data have also been shown to be more frequent in this phase (Azorin-Molina et al., 2021).

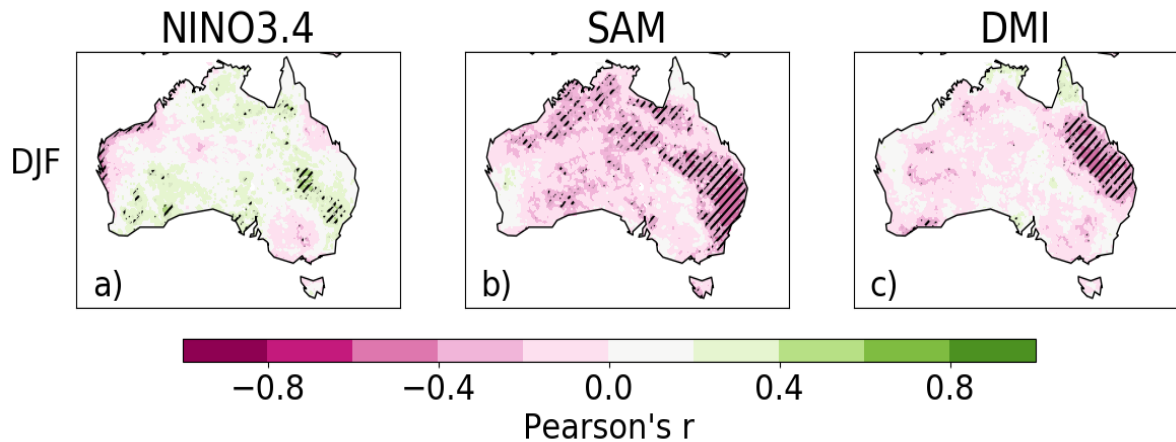


Figure 4.1: Correlations for summer between the number of days with a favourable severe convective wind environment and seasonally-averaged indicators of a) ENSO (Niño3.4 index) b) IOD (Dipole Mode Index) and c) SAM (Marshall Index) for 1979-2018. The thunderstorm environments are calculated from the ERA5 reanalysis (Hersbach et al. 2020) based on the method of Brown & Dowdy (2021). Hatched regions indicate a significant relationship at the 95% confidence level (e.g., about 5% of the region could be expected hatched on average due to random chance alone). NINO3.4 and DMI data are attained from the NASA ESRL (https://psl.noaa.gov/gcos_wgsp/Timeseries/) while SAM data are from <https://legacy.bas.ac.uk/met/gjma/sam.html>.

Other phenomena that can cause severe wind gusts

Phenomena other than thunderstorms can produce severe wind gust speeds in some cases, including TCs in the more northern regions of Australia (with relatively little influence on central-east regions of Australia), as well as ECLs in near-coastal regions in the southeast and eastern of Australia while noting that the most damaging ECLs typically occur during the cooler months of the year (which reduces their relevance to this study's application here for summer). Long-term climate trends in the occurrence of TCs and ECLs and associated severe wind gusts during the summer months are briefly discussed here, including in relation to a changing climate, while noting that the primary focus of the analysis here is on severe thunderstorms for the purposes of this study.

Fewer ECLs are projected in a warming world, but with higher confidence during the cooler months of year and more uncertain changes projected in the future occurrence of ECLs during summer (Dowdy et al. 2019a). This includes large uncertainties around the projected change in the intensity of intense ECLs during summer (i.e., those with extreme wind speeds).

The topic of TCs and associated severe wind gusts has received widespread attention in Australia, including in relation to building codes and Australian structural design standards. Wang et al. (2013) reported that structures along the north-east coast of Australia may already be subject to higher gust speeds than the current design standard permits, with projected changes in severe wind gust speeds being sensitive to TC frequency and intensity change, particularly between Cairns and Townsville.

There has been a significant downward trend in the occurrence frequency of TCs observed in the Australian region (Dowdy 2014; Chand et al. 2019). Future projections based on global models are consistent with these findings in indicating a downward trend in the occurrence frequency of TCs in the Australia region (Bell et al. 2019). The currently available range of climate models have large uncertainties in their simulations to identify the more intense and damaging TCs (e.g., Category 4-5) such that there is considerable uncertainty in

future changes in damaging wind speeds associated with them (Knutson et al. 2020; NESP 2020). Observational studies indicate that for the east coast of Australia there has been no change in severe landfalling TCs (Chand et al. 2019), with an increase suggested by Holmes (2020) primarily since 2011 and mostly evident between Townsville and Rockhampton (noting that this is a relatively short time period for climatological assessments of rare events with large interannual variability such as these). A recent review that considered observations and future projections concluded that the frequency of Category 4 and 5 TCs may not change or increase slightly along with some poleward migration or little change in their spatial extent being plausible future outcomes, but with considerable uncertainties, as detailed in NESP (2020).

To summarise for TCs, the rareness of category 4-5 TC events and relatively short historical time period for high-quality observations embeds a considerable degree of uncertainty on how climate change could influence TC-related wind gust risk on the northeast coast of Australia, especially at the regional level. By considering the available information including from modelling and observations, it can be said with low-medium confidence that little change or an increase are more likely than a decrease in the occurrence frequency of Category 4-5 TCs in the future for Australia, including for the east coast during summer.

4.3 Summaries for historical information

Observed trends

Because of observational constraints, historical trends in the frequency and intensity of convective winds in Australia are unknown (Walsh et al. 2016; Brown & Dowdy 2019). This is largely due to spatio-temporal inhomogeneities in severe weather reports (Allen et al. 2011) and wind observations (Jakob 2010). It is also noted that convective phenomena occur on small spatial scales which are often missed by the observational network and make the detection of trends difficult. However, observed lightning activity, indicative of convective activity, indicates a potential long-term decrease in occurrence frequency during winter in southern Australia with little change during summer (Bates et al. 2015).

More broadly, extreme winds from station data (defined as the 90th percentile of daily maximum observations and including all wind-producing phenomena) have shown long-term decreases in frequency in Australia (Azorin-Molina et al. 2021), consistent with decreases in average wind gust magnitude (McVicar et al. 2008). These changes may be partly attributable to environmental factors such as vertical wind shear and thermal instability, although the exact causes are unknown. Further details on trends are provided in subsequent sections below, including for studies based on reanalyses.

Model assessment

GCMs, reanalyses and commonly used downscaling approaches available for Australia are unable to resolve the small spatial scales required for simulation of SCWs. Therefore, models are assessed here in terms of their ability to correctly represent the environments which are favourable for SCW occurrence, as well as the spatial and temporal variability of these environments. In addition, the ability of environmental model diagnostics to represent the variability of observed events is discussed.

For Australia, GCMs are generally able to represent the spatial distribution of severe thunderstorm environments, although significant biases may exist for individual models in the seasonal and diurnal cycle, related to the representation of near-surface moisture (Allen et al. 2014). In other regions, climate model representation of thunderstorm environments has been shown to vary greatly with individual models (Seeley & Romps 2015), while some models

have been shown to replicate historical trends in environments for sufficiently large climate signals (Pistotnik et al. 2016). Individual model biases for severe thunderstorm environments may be addressed to some extent using a multi-model ensemble with bias correction.

Reanalysis models used for historical analyses can reliably represent atmospheric environments based on observed sounding data (Brown & Dowdy 2021), although some key elements such as CIN may remain unresolved due to insufficient vertical resolution (King & Kennedy 2019). SCW diagnostics from these models can broadly represent the seasonal and diurnal cycle of measured wind events in Australia (Brown & Dowdy 2021). Diagnostics have also been shown to have a statistically significant correlation with the observed inter-annual variability of SCW events, which has also been found for other small-scale convective hazards in other regions, such as tornado events in the United States (Gensini & Brooks 2018). In addition, environmental model diagnostics have been shown to explain most of the variability in convection resolving model thunderstorms (Hoogewind et al. 2017).

In summary, atmospheric models which use historical observations (reanalyses) can reliably represent thunderstorm environments, and diagnostics intended to identify SCW environments are able to broadly represent the variability of observed events. Significant biases exist in the representation of these environments within individual climate models, although biases may be somewhat addressed using multi-model ensembles with bias correction.

Trends in severe convective gust environments

Historical trends in the frequency of atmospheric environments favourable for SCWs are assessed here using the ERA5 reanalysis (Hersbach et al. 2020). As described in sections above, environmental approaches such as this are common for assessing convective hazards in model data, including for long term trends (Rädler et al. 2018; Taszarek et al. 2020).

Figure 4.2 presents historical summertime trends from 1979-2018, using four different diagnostics for environment identification. This includes one diagnostic which has been developed by Brown & Dowdy (2021) using statistical methods (referred to herein as the Brown Dowdy Statistical Diagnostic: BDSD, as well as three other diagnostics that have been used in a range of previous studies and for severe weather forecasting purposes. The BDSD was shown to provide a good representation of spatial and temporal variability in observed convective wind events as compared to other commonly used environmental diagnostics for severe thunderstorm environments, with further details on these diagnostics and analysis available in Brown & Dowdy (2021).

The BDSD indicates little to no long-term trend in occurrence frequency for southeast Australia (Figure 4.2). There are some areas of decreasing frequency over inland regions, broadly consistent with previous results for the state of South Australia noting some fine-scale regional variations (Brown & Dowdy, 2019). These areas of decreasing frequency for BDSD also appear when considering the other diagnostics shown in Figure 4.2. These alternative diagnostics also indicate some areas of increasing frequency off the south-east coast. That increase is broadly consistent with previous analysis of thunderstorm environments indicating positive trends in this far-southeast region with negative trends in general for other regions including northern Australia (Dowdy 2020a).

The BDSD is specifically tailored to SCW environments and designed to represent a broad range of relevant physical processes (e.g., a broader range of processes than is the case for the other diagnostics shown in Figure 4.2). However, the other diagnostics are also considered in this analysis for general completeness, as well as noting the considerable uncertainties around the use of any single method for analysis of long-term climate trends in SCWs based on currently available knowledge.

In summary, this trend analysis based on reanalysis data indicates relatively little change throughout most of southeast Australia including based on the BDSD statistical method, with a potential increase indicated for some near-coastal regions in the far southeast in near-coastal regions from the full set of diagnostics more broadly (while noting low confidence in general). Decreases are indicated for most northern and eastern regions, with increases also indicated for some southwest regions of Australia.

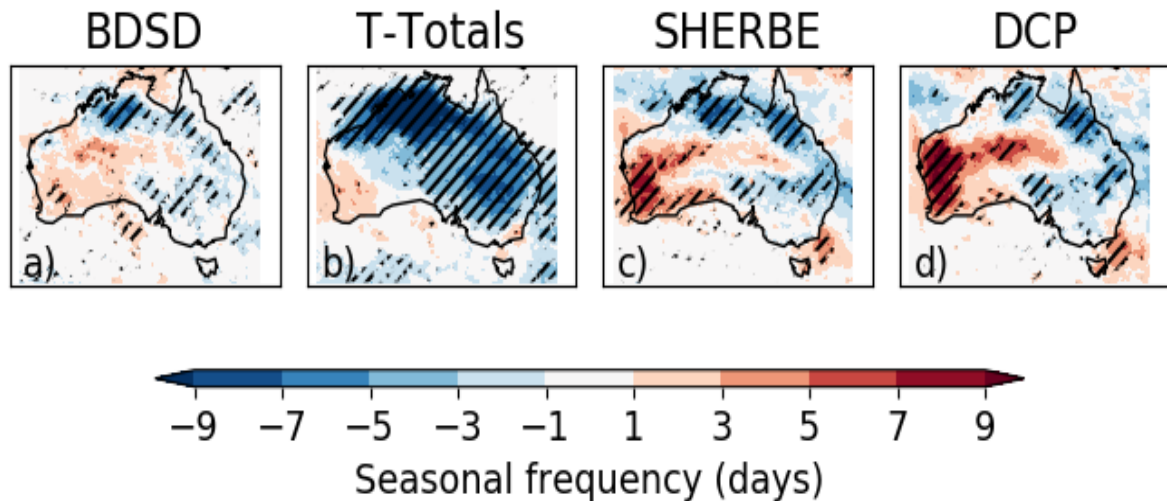


Figure 4.2: Long-term changes in the frequency of days with favourable SCW environments during the summer, based on ERA5 reanalysis data. Changes are based on four diagnostics, (a) BDSD, (b) total totals (T-Totals), (c) severe hazards in reduced buoyancy environments (SHERBE) and (d) the derecho composite parameter (DCP). The change in the mean number of days per season is shown, calculated as the difference from the period 1979:1998 to the period 1999:2018. Significant changes are represented by hatching based on Student's t-test with a 90% confidence level (two-tailed).

4.4 Summaries for projected changes

Global climate models

As discussed in sections above, there is very limited information available on projections of SCWs in Australia. Here we use various environmental diagnostics (as used to assess historical trends in Section 4.3) applied to future projections data from a bias-corrected 12-member CMIP5 ensemble (Taylor et al. 2012).

Future changes in the frequency of environments are presented for four diagnostics relevant for convective winds between 1979-2005 and 2081-2100, presented for the summer months December to February (Figure 4.3). These diagnostics are the same as those used in Section 4.3, again noting that the BDSD (Figure 4.3a) is potentially most suitable based on representing the variability of historical events (Brown & Dowdy 2021). The BDSD generally indicates increases in the frequency of environments across Australia, although little or no change may be more plausible for some near-coastal regions in eastern Australia and Tasmania. Increases are also generally indicated for two of the other three diagnostics (SHERBE and DCP), while decreases are indicated by the total totals diagnostic. The diagnostics which indicate increasing frequency in environments are largely driven by increasing moisture content in the lower atmosphere, while the decrease for total totals is driven by a stabilisation of the temperature lapse rate. Increasing moisture and decreasing lapse rate are expected in the

future (see Section 4.2) and have opposite effects on the potential for convection to occur. These competing factors introduce uncertainty for future projections of SCW environments as represented by these diagnostics, as it is unclear whether changes to the atmospheric lapse rate or moisture will be more influential.

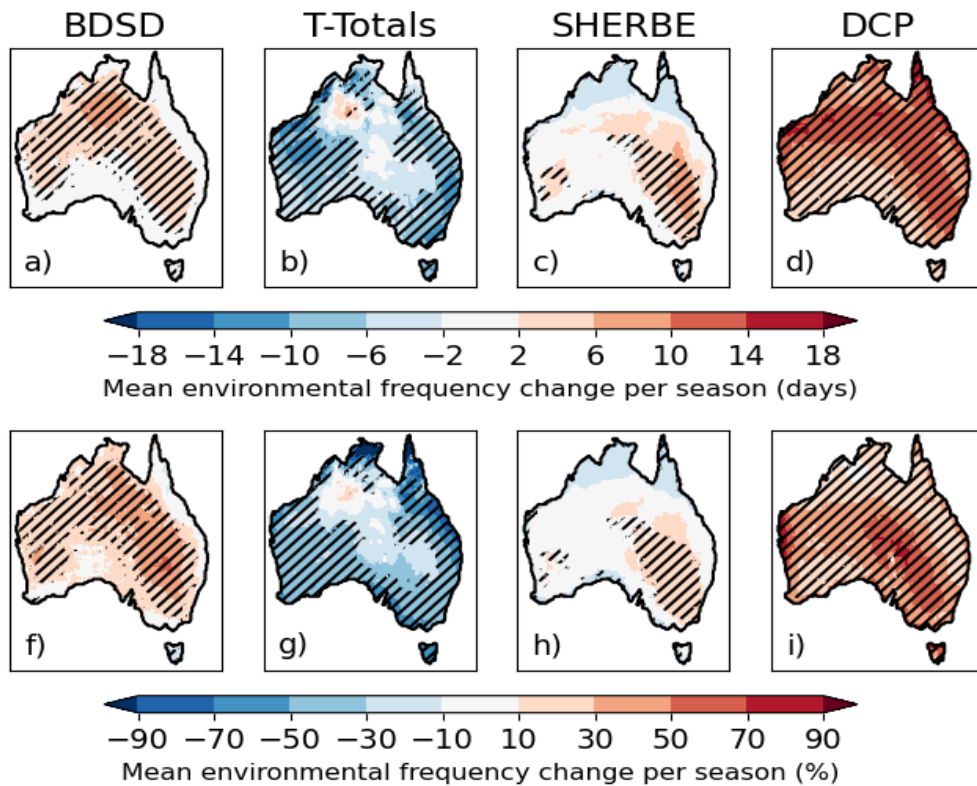


Figure 4.3: Projected future changes in the frequency of favourable SCW environments during summer shown as (a-d) a change in the number of days per season and (f-i) percentage changes. The changes are calculated from the period 1979:2005 to the period 2081:2100 based on a high emissions pathway (RCP8.5) using an ensemble of 12 GCMs. The ensemble median response is shown. Changes where at least 10 (out of 12) models agree on the sign of change, as well as where the seasonal mean number of environments in the historical period is greater than one, are shown with hatching. These results are intended for broad-scale guidance on some of the plausible changes that could occur for SCW occurrence in a warmer world, including on direction of change and estimated range of potential future change as represented by these metrics.

Convection-permitting modelling

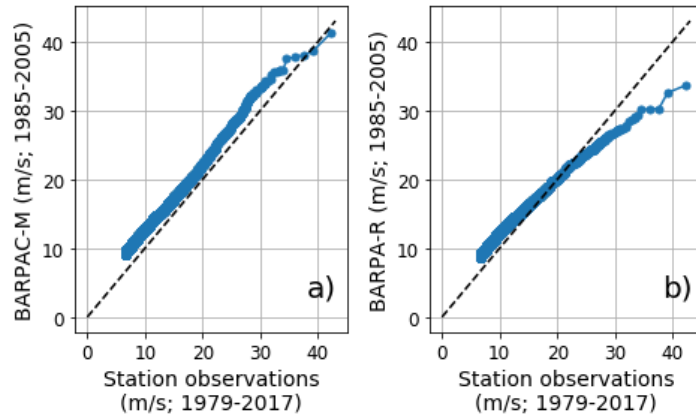
Convection-permitting modelling has been used in a relatively limited number of studies as an alternative to the large-scale environmental approaches commonly used for projections of severe thunderstorms and associated hazards. Although being very computationally expensive, this type of modelling can have the advantage of simulating some factors which are more challenging to represent in environmental approaches. This can potentially include better simulation of CIN and some triggering mechanisms such as the influence of localised orographic features, as well as potential for improved representation of some other aspects of thunderstorm characteristics (e.g., potentially providing some estimates of intensity and morphology in some cases).

Leslie et al. (2008) used a convection-permitting model to dynamically downscale climate model data in order to study potential future changes to hailstorms in Sydney, with results suggesting an increase in the number of large hail events but with little change to the total number of hail events. Although there have not been any subsequent studies which have built on those results for Australia, modelling in the United States has found similar increases for large hail with little change or decreases for moderate- and smaller-sized hail (Trapp et al. 2019; Raupach et al. 2021). There have also been modelled increases for the frequency of hazardous convective events in general without being specific on the type of hazard (Hoogewind et al. 2017). Elsewhere, convection-permitting modelling in the United Kingdom has suggested an increase in the intensity and frequency of convective rainfall (Kendon et al. 2017). However, more modelling at these fine scales, including with a greater number of driving GCMs and covering longer periods needs to be done to build on these results, including with a focus on severe thunderstorms in Australia's changing climate.

A limited amount of convection-resolving modelling was produced for this project by applying the BARPA modelling framework using around 4 km horizontal grid spacings, covering a reduced mid-latitude domain including the capital cities of Sydney, Adelaide, Melbourne and Hobart (as well as noting the availability of BARPAC-T using a 2 km grid spacing for a region around the tropical east coast of Australia). Initial results suggest that this convection-resolving approach which includes downscaling the ACCESS1-0 GCM (BARPAC-M) can provide a better representation of severe wind gusts relative to the convection-parameterising BARPA configuration (BARPA-R) that has a 12-km horizontal grid spacing. For example, analyses of BARPAC-M and BARPA-R data are presented here and compared with daily maximum wind gust observations from station data at 12 locations (Figure 4.4a,b), indicating broadly similar results for BARPAC-M to those based on observations with somewhat lower wind speeds for the upper tail in BARPA-R. These 12 locations are from observation stations in the BARPAC-M region that have a reasonable quality and length of wind data suitable for climate analysis, such as discussed in Brown & Dowdy (2021).

Results also suggest that the BARPAC-M model under a future climate scenario (2039-2059) produces stronger 20-year maximum wind gusts when considering all land points in the domain relative to the historical run (1985-2005; Figure 4.4c). These results for future changes may not be statistically significant due to the small sample size of extreme gusts and noting various uncertainties from the modelling approaches (including potential variation between different host models, time periods, emission pathways, etc.), the gust origins (i.e., synoptic or convective, as well as potential for different types of convective modes) or spatial variations. However, they demonstrate that convection-resolving approaches may provide additional insight into future changes in extreme events such as SCWs. In particular, these initial results indicate that increased intensity of SCWs in the future is one plausible outcome, while noting the considerable uncertainties discussed above and the limited data currently availability for convection-permitting modelling of future simulated climates.

Daily maximum wind gust QQ-plot at 12 locations (m/s)



Maximum 20-year wind gust QQ-plot over all land grid points

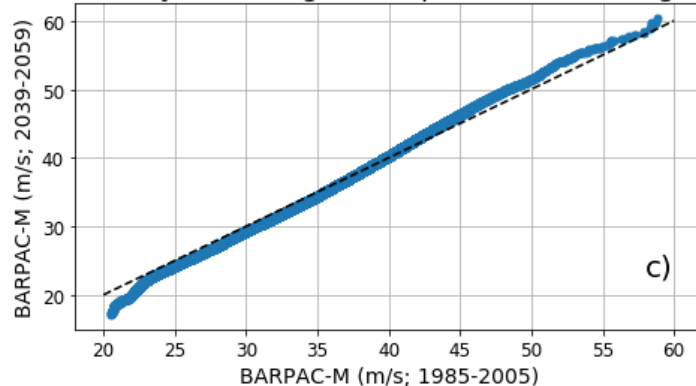


Figure 4.4: Modelled wind gust speed vs observed wind gust speed, presented for different quantiles of daily maximum wind gusts at 12 locations. Results are presented from the convection-permitting mid-latitude model run of BARPAC-M (a) as well as from its host model for the regional configuration of BARPA-R (b). As one example of projected future changes based on BARPAC-M, the 20-year maximum wind gust is shown under historical (1985-2005) and future (2039-2058) conditions, with the blue line representing the quantile-matching of wind speeds between those two periods using data for individual grid points (land only). The dotted line represents no change from historical to future, with values below and above that line representing decreases and increases, respectively, in the occurrence frequencies of wind speeds in the ranges shown.

4.5 Lines of Evidence Table

Table 4.1: Lines of Evidence Table for severe convective winds (SCWs), with a focus on summer in the southeast and east of Australia. The degree of influence is listed in black, followed by whether this information implies an increase (red), decrease (blue) or little change (black) in the occurrence of SCWs, as well as by increased uncertainty (purple) in the direction of change. The rows of information are not in order of importance.

Physical processes and their measures	
Thunderstorm environments (not specific only to SCWs)	Medium-Strong association. More favourable environments in parts of southeast (low confidence) with increasing moisture content (high confidence), as well as decreasing atmospheric lapse rate (medium-high confidence) and vertical wind shear (medium confidence).
SCW environments	Strong association. Many uncertainties and few studies to date.
Thunderstorm initiation	Strong association. Uncertain changes (relating to extratropical cyclones, fronts, jet-streams, atmospheric waves, orographic flows and convective inhibition).
ENSO	Weak association. Uncertain future change.
IOD	Weak association. Uncertain future change.
SAM	Moderate association in eastern Australia. Projected shift towards positive SAM.
Additional factors including phenomena such as cyclones	Moderate influence of TCs in subtropics, as well as ECLs in coastal east and southeast, for damaging winds in summer. Uncertain expansion of TC range. Fewer TCs, but potentially more intense on average. Uncertain projections for summer ECLs, including intensity and associated extreme winds.
Assessment for historical period	
Model assessment	SCW environments can be simulated reasonably well by calibrated climate model ensembles, while noting many other uncertainties.
Historical trend in SCW environments	Little change or fewer through inland eastern Australia, small region of potential increase in south-east (low confidence, with uncertainty in modelling methods and limited observations).
Historical trend in observed SCWs	Uncertain due to observational constraints.
Projected future change	
GCMs	More SCW environments for southern and eastern Australia (low confidence due to uncertainty in model diagnostics).
RCMs and convection-permitting models	Some indication of a potential increase , but with very limited available data and analysis to date (highlighting a need for more research).

4.6 Projections Likelihood Information

The lines of evidence table (Table 4.1) shows high uncertainty in observed trends and projected future changes for SCWs, with additional uncertainties around projected changes of related physical processes for extreme winds during summer in the southeast and east of Australia. A considerable amount of this uncertainty arises from the small spatial scales associated with the physical processes that lead to the occurrence of severe thunderstorms and the SCWs they can cause, resulting in a limited ability to model these events based on current approaches (while noting some potential improvements using convection-permitting modelling). Uncertainty also arises from the lack of suitably homogenous observations for long-term climate trend analysis.

Some insight on plausible future changes is provided by the environmental diagnostic approach (i.e., large-scale diagnostics). Calibrated model projections from an ensemble of GCMs indicate a range of plausible changes (including increases and decreases) in the frequency of days with favourable conditions for SCWs, with ensemble median estimates of a 7% and 8% increased frequency for southern Australia and eastern Australia, respectively,

based on the supercluster regions defined in CSIRO & BoM (2015). Confidence in this result is relatively low (i.e., much lower than for extreme temperature projections from the previous section) and spans a wide range of plausible change indicated by the different diagnostics and individual GCMs (e.g., 10th and 90th percentile estimates based on a 48-member model-diagnostic ensemble provided in Table 4.2). Increasing environmental frequency based on median estimates agrees with expected changes to thunderstorm environments in Australia based on physical process understanding (*Low Confidence*), including increased atmospheric moisture content in a warmer world, although decreases are also plausible due to decreasing atmospheric lapse rates (as indicated by one of the diagnostics in Figure 4.4: Total-Totals) as well as noting uncertainties relating to factors not included in these environmental diagnostics (e.g., initiation mechanisms and convective inhibition).

The results based on environmental diagnostics are broadly similar to the initial results from the convection-permitting model runs of BARPAC-M, which indicated a small increase in the upper tail of wind gust speeds in the future. However, further research is required to examine how well these extremes can be simulated in the fine-scale model data provided by convection-permitting dynamical downscaling modelling approaches.

In summary, an increased occurrence frequency of severe winds is indicated in the southeast and east of Australia during summer but with low confidence, noting that both increases and decreases are plausible outcomes based on the full range of lines of evidence considered here. The estimated range from the environmental modelling (Table 4.2) is intended to be useful for some planning and risk management purposes. The central estimates of the model ensemble could also be useful in some cases, showing that the most likely projections for the future is little change or a small increase in frequency (*Low Confidence*).

Table 4.2: Projected percentage changes in severe convective wind environment frequency (days per season) during summer, based on 12 CMIP5 GCMs, as well as using four diagnostics (Brown & Dowdy 2021). This results in a 48-member ensemble, with the median, 10th and 90th percentile changes shown. The changes are calculated from the period 1979:2005 to the period 2081:2100 based on a high emissions pathway (RCP8.5), averaged over Eastern and Southern Australia (using the regions defined in CSIRO & BoM (2015)).

NRM super-cluster region	Median change	10 th percentile	90 th percentile
Eastern Australia	8%	-56%	33%
Southern Australia	7%	-49%	45%

5. Method application: extreme bushfire weather conditions

5.1 Introduction

Bushfires can be considered as a form of compound event given the range of factors that influence their occurrence, including based on the combined range of weather factors that can influence their occurrence (from various near-surface conditions to higher-level atmospheric processes including convection through the troposphere and into the stratosphere in some extreme cases). In addition to the combination of various weather conditions, the occurrence of dangerous bushfires can also be influenced by various other factors including vegetation conditions (such as relating to fuel load and type) and ignition sources (such as associated with human activities or with lightning), some of which can be challenging to incorporate into integrated frameworks for modelling of compound events (e.g., given the current limitations in coupled fire-atmosphere-vegetation climate modelling). Although there are very large uncertainties around modelling fuel conditions and ignition sources including in a changing climate, these other factors are also considered in this section, while noting that the primary focus of this analysis is on dangerous weather conditions for bushfires.

Bushfire weather conditions are often represented by indices as a useful way of combining various weather conditions known to influence fire behaviour (e.g., near-surface humidity, wind speed, temperature and rainfall). Examples of such indices include the Forest Fire Danger Index (FFDI) commonly used in Australia (McArthur 1967) as well as the Fire Weather Index (FWI) originally developed in Canada but now widely used throughout the world (Van Wagner 1987; Dowdy et al. 2009; Field et al. 2017). The FFDI and FWI are both based on near-surface measure of humidity, wind speed, temperature and rainfall, with a broadly similar order of sensitivity to these four individual weather conditions (Dowdy et al. 2009). Indices have also been developed for grass fires, such as the GFDI (McArthur 1967), while noting that grass fires were not identified by the energy sector stakeholder for this research as a significant hazard. Indices are also available for various other fuel types including a multi-index system currently in development for Australia (known as the Australia Fire Danger Rating System: AFDRS). Indices such as the Continuous-Haines index (C-Haines) are based on conditions at higher levels of the atmosphere and can be useful for indicating risk factors associated with the occurrence of extreme fire events (including very dangerous fires that generate thunderstorms in their fire plumes known as pyrocumulonimbus or pyroCb clouds) (Mills & McCaw 2010; Dowdy & Pepler 2018; Di Virgilio et al. 2019; Dowdy et al. 2019b). Many of the more disastrous fire events in recent decades have been associated with the occurrence of pyroCb events, including for the Canberra fires in 2003 and the Black Saturday fires in 2009 as well as during the 2019/2020 Black Summer fires (Fromm et al. 2006; Cruz et al. 2012; McRae et al. 2013; Dowdy et al. 2017; Australian Government 2020).

The SMPL is applied here for extremely dangerous fire weather conditions during summer in the southeast and east of Australia, considering some similar aspects to those detailed in Sections 3 and 4. However, in contrast to the application of this method for individual weather conditions such as extreme temperature (Section 3) and extreme wind speed (Section 4), the combined influence of multiple different weather conditions known to influence fire behaviour is considered here. Factors considered include near-surface weather variables such as humidity, wind speed, temperature and drought measures relating to fuel availability, as well as other atmospheric phenomena such as the influence of synoptic systems, mesoscale convective processes as well as large-scale atmospheric and oceanic modes of variability. Although the focus here is on fire weather, other factors relating to bushfire occurrence are also discussed including ignition and fuel conditions.

5.2 Summaries on physical processes

Individual weather factors

Weather conditions such as humidity, wind speed and temperature can influence fire behaviour in Australian forests (McArthur 1967), with the conditions changing as our climate warms (CSIRO & BoM 2015; BoM & CSIRO 2020). As detailed previously for extreme temperature (Section 3), climate change is increasing the frequency and severity of extreme heat events (*high confidence*), including for individual days as well as for more prolonged events (e.g., heatwaves). This is based on many lines of evidence including from observations, modelling and physical processes understanding.

Observed changes in humidity across Australia are not well described by linear trends over time, but most sites across Australia have shown long-term increases in atmospheric water vapour concentrations (i.e., including measures of this such as dewpoint temperature and specific humidity), with the largest increases in the interior of the continent and some eastern regions (Lucas 2010). Increased temperatures lead to an increase in the moisture holding capacity of the atmosphere (of about 6-7% per degree of warming based on the Clausius-Clapeyron relation), which results in increased water vapour pressure in general (i.e., increased specific humidity). However, it is relative humidity (or vapour pressure deficit) that is important for fire behaviour including given its influence on fuel moisture, noting that relative humidity depends on both water vapour pressure as well as air temperature. As some regions warm faster than others (e.g., land regions warm more than ocean in general) there can be differences in the relative humidity for a given change in water vapour content. In general for Australia, a decrease in relative humidity is projected to occur, including during summer with CSIRO & BoM (2015) listing *medium confidence* for this (as compared to *high confidence* for winter and spring), while noting some finer-scale modelling from RCMs indicates little change in some regions (Clarke & Evans 2019).

A small decrease in wind speed has been observed for Australia in general, while noting considerable uncertainties relating to data availability and homogenisation (Azorin-Molina et al. 2021). There are also considerable uncertainties around model data for wind speed, including due to significant negative bias in modelled wind speed during high wind conditions (in general for most models). Many factors such as boundary layer mixing, form drag for sub-grid orography and surface properties can influence wind estimation over land. The representation of the stable boundary layer remains challenging due to the multiplicity of physical processes (including turbulence, radiation, land surface coupling and heterogeneity, turbulent orographic form drag) involved and their complex interactions, such that models typically suffer biases in wind speed under such conditions. Projections for Australia indicate little change or a small decrease during summer in mean wind speed, with considerable variation between different models: some show increases and others show decreases, typically within about +/-5% in magnitude (CSIRO & BoM 2015). Further details on processes that can cause strong winds are provided below in this section (in relation to synoptic-scale phenomena such as fronts and blocking highs).

Drought and fuel moisture

Drought conditions can lead to low moisture content in vegetation that increases the availability of fuel for bushfires. Climate change is expected to increase the intensity, frequency and duration of meteorological drought (i.e., a measure of drought based only on rainfall deficit), including based on longer periods with little rainfall as detailed in CSIRO & BoM (2015). It is also noted that there are various other ways that drought conditions can be defined including agricultural drought measures that can include the influence of other weather

conditions (e.g., temperature, humidity, wind as well as evapotranspiration) in addition to rainfall.

Fire weather indices such as the FFDI and FWI include drought measures in their formulation that are more similar to measures of agricultural drought than meteorological drought in that they include the influence of other weather conditions in addition to rainfall. For example, temperature is used together with rainfall as input to the Keetch-Byram Drought Index (KBDI) (Keetch & Byram 1967) as often used as an input for the Drought Factor used in the FFDI (noting that indices relating to soil moisture such as KBDI are used for the Drought Factor to indicate a proxy estimate of fuel availability based on moisture content). In contrast, relative humidity, temperature and wind speed are used for the multiple different fuel moisture measures that the formulation of the FWI System includes (Van Wager et al. 1974). Consequently, in addition to rainfall and meteorological drought a broader range of factors can be considered when examining potential future changes to fuel moisture content.

As noted in the section above on individual weather factors, mean temperatures as well as the frequency of extreme temperature events are projected to increase in the future with high confidence, together with a general decrease in relative humidity, as well as little change or a small decrease in wind speed. Considering these factors together with the projected increase in meteorological drought (including increased frequency, intensity and duration) suggests a likely increase in the frequency of very dry fuel conditions. However, there are considerable uncertainties around projected changes in different types of drought as well as fuel moisture responses to climate change, including as noted in Section 3 in relation to soil moisture projections. Regional models may add value for some of these factors (e.g., more detail on land surface processes, rainfall and orographic dependencies).

Combined weather conditions

Fire weather indices provide a useful way to combine a range of weather conditions known to influence fire danger. The index values are typically calculated for each individual time step (e.g., day) using data for each weather factor obtained from a single model (as is the case for all results and references described in this report). This ensures the coherence of these individual weather factors when applied for individual time steps from a single model. After the fire weather index values have been calculated for each model, the ensemble statistics and other derived products can then be produced, rather than using ensemble average values of individual weather conditions as input to calculate the fire weather indices as that will lose the coherence of individual weather factors (including noting the importance of this for representing extremes of the fire weather index values). Similarly, the weather data should be calibrated prior to calculating the fire weather indices, rather than calibrating the resultant index values, to keep the relative balance of each weather factor correct for the index formulation.

The Forest Fire Danger Index (FFDI) is commonly used in Australia as a general indicator of regional weather features associated with dangerous fire conditions. It shows broad similarities to some other fire weather indices used around the world such as the FWI including for its sensitivity to different input ingredients (including being most sensitive to wind speed followed by humidity and then temperature) (Dowdy & Mills 2012). Observational studies have identified an increase in both the average FFDI and the frequency of high FFDI days over much of southern Australia, particularly during the spring months, contributing to a lengthening of the fire season (Dowdy 2018, Harris & Lucas 2019). These trends are attributable at least in part to anthropogenic climate change, including as they combine several different weather variables of which some (temperature) can be more easily attributed to climate change than others (humidity and wind). Although a significant climate change signal

is able to be demonstrated already based on observations (Dowdy 2018; Harris & Lucas 2019), the attribution of individual fire events to climate change is more challenging while noting one recent study that has done this for the Black Summer of 2019/2020 (van Oldenborgh et al. 2021).

Projected changes in extreme daily FFDI were recently produced for Australia drawing on a comprehensive range of modelling techniques, comprising an ensemble of projections based on GCM output as well as two ensembles of projections based on dynamical downscaling using regional model approaches (Dowdy et al. 2019b). Those projections indicate an increase in the number of days with very high fire weather conditions (based on FFDI above 25) as well as an increase in the number of days with FFDI above the 95th percentile for 1990-2009), noting lower agreement between models in some parts of eastern Australia. Similarly, future increases were also projected for the number of days with FFDI above 50 and for the number of days with FFDI above the 99th percentile for 1990-2009 (Dowdy 2020b). In addition to the projections presented in those studies, plausible variation above and below such values is indicated from previous studies based on different metrics and different modelling approaches using FFDI. For example, relatively large increases have been derived using monthly mean climate changes from 3 GCMs to scale observations and calculate changes in severe fire weather days with FFDI > 50 (CSIRO & BoM 2015), as well as other studies that indicate less confidence in large increases in FFDI in the future (Clarke et al. 2016).

Projections of future climate have also been produced based on other fire weather indices, including a global study that used the FWI (Abatzoglou et al. 2019) and reported no emergent climate change signal in general for Australia based on the methods they presented. Although increases were projected in some regions they were not statistically significant at a high confidence level noting the high interannual variability that can occur in weather and climate conditions in Australia (such as due to the influence of large-scale modes of variability including ENSO, discussed in sections below). Examples such as this based on FWI with little change indicated, together with the range of FFDI projections from various studies noted above, show that considerable differences can occur between different studies and highlight the benefit of considering a broad variety of datasets, methods and studies (as is a goal of the method applied here).

Very dangerous types of fire events have also been examined in relation to climate change, including extreme pyro-convection conditions (i.e., associated with thunderstorms that form in fire plumes: pyroCbs). These occurred for the Black Saturday fires in 2009 and the Canberra fires in 2003 fires as well as many examples during the 2019/20 Black Summer fires (Fromm et al. 2006; McRae et al. 2013; Dowdy et al. 2017; Australian Government 2020). Significant trends have been found for extreme pyro-convection risk factors including based on historical data (Dowdy & Pepler 2018) and future projections (Di Virgilio et al. 2019; Dowdy et al. 2019b). These studies indicate increased risk factors for parts of southern and southeast Australia as well as decreases in some cases for other regions, including in parts of eastern Australia. However, a range of uncertainties around future changes in convective systems is also noted, such as the contrasting roles of increasing water vapour content and decreasing lapse rates that can have various influences on risk factors associated with fire behaviour and/or potential for convective systems to develop (with details also available in Section 4 around uncertainties in future projected changes for convective systems).

Subtropical ridge; Blocking/high pressure systems; Cold fronts

Details on various phenomena including the subtropical ridge, blocking highs and cold fronts were provided previously (see Section 3), including observed and projected changes

during summer, as well as strengths and limitations of different modelling approaches. Building on that information for those phenomena, details specific to fire weather conditions are provided in this section.

The projected increase in the strength of the subtropical ridge could potentially act to exacerbate the severity of some fire weather events in the future, especially in parts of southern Australia. For example, the high-pressure systems that characterise the subtropical ridge can lead to descending dry air and clear skies associated with hot and dry conditions. High pressure systems can also circulate air around inland Australia in some cases, as a dynamical mechanism contributing to the build-up of extremely hot and dry air, while noting it is not currently known if this process would change in the future.

Blocking (quasi-stationary) highs over the Tasman Sea can advect hot and dry air from inland regions towards the more densely populated regions closer to the south and east coasts. They can also interact with approaching cold fronts from the south which can intensify wind speeds and contribute to increased severity of fire weather conditions in some cases. In particular, the most severe fires in southeast Australia are typically associated with a strong cold front approaching from the southwest, often with a high in the Tasman Sea, producing very hot, dry and strong northwesterly winds in southeast Australia corresponding to very dangerous fire weather conditions (Hasson et al. 2009; Reeder et al. 2015; Dowdy et al. 2017). The passage of the front (or pre-frontal trough) comprises shifts in wind direction which can change the direction of fire movement, i.e., the northern flank can become the new head fire leading to rapid increases in the rate of area burnt. This can cause significant challenges for firefighters (Cruz et al. 2012). While future projections of blocking and cold fronts are generally uncertain, as detailed in Section 3, one study based on the older generation of climate models (CMIP3) found a projected increase in frequency of such extreme events from 0.5 to 1-2 per year by the end of the 21st century (Hasson et al. 2009).

Modes of variability – ENSO, IOD and SAM

Details on modes of variability including ENSO, IOD and SAM in a changing climate were provided in Section 3. Building on that information, aspects relating to fire weather conditions are summarised here.

A recent paper summarised the seasonal influences of these three modes of variability on average fire weather conditions in Australia (Harris & Lucas 2019), finding a strong influence from ENSO during spring and summer in the east, from IOD during spring in the southeast and east and from SAM during spring and summer in the east (with negative SAM associated with more severe fire weather conditions such as in 2019/20). This is broadly similar to various other studies that have also examined some of those aspects (Dowdy 2018; Abram et al. 2021). Out of 21 significant bushfire seasons since 1950 in south-east Australia, 11 were preceded by a positive IOD (Cai et al. 2009). In Victoria, particularly spring, a positive IOD contributes to lower rainfall and higher temperatures, exacerbating dry conditions and increasing the fuel availability leading into summer.

Sudden stratospheric warmings can also influence fire weather conditions in Australia, including hotter and drier conditions for parts of eastern Australia during spring and early summer which could also influence fuel moisture content during summer to some degree, noting that the influence of such events can also be indicated through the SAM index (given the association between polar stratospheric vortex conditions and measures of the Southern Annular Mode) (Lim et al. 2019; 2021). The influence of climate change on sudden stratospheric warming events is currently unknown.

Although the relationships between fire weather and modes of variability (including ENSO, IOD and SAM conditions) have been examined in numerous previous studies (such as those discussed in this section), this has not previously been examined in detail for more extreme measures of fire weather, such that some new analysis on that is shown in Figure 5.1. Correlations are presented between the number of days with $\text{FFDI} > 99.5^{\text{th}}$ percentile and various modes of variability (using indices representing ENSO, SAM and IOD) showing broadly similar features to those for average values of fire weather measures as described based on previous studies mentioned above. In particular, fire weather conditions in the southeast and east of Australia during summer show relationships with ENSO and IOD (significant positive correlations), with SAM having some influence in central east regions (positive correlation) but to a lesser degree than ENSO and IOD. There are some regions of negative correlation for the SAM results in the more inland parts around central-east and southeast Australia, but those correlations are not statistically significant. It is also noted that the influence of sudden stratospheric warmings (relating to negative SAM conditions to some degree) can be associated with more severe fire weather conditions in central eastern Australia during spring (Lim et al. 2019), with this not expected to be represented in these results focussed on summer.

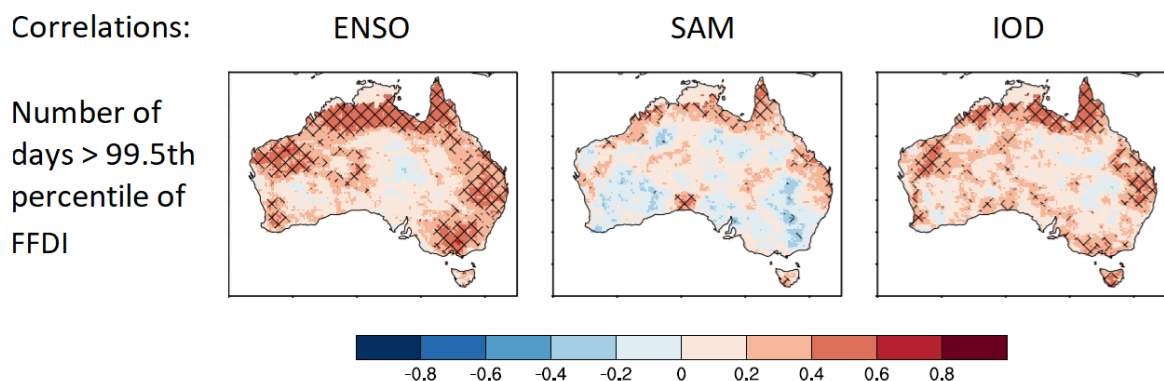


Figure 5.1: Correlations for the number of days with $\text{FFDI} > 99.5^{\text{th}}$ percentile during summer and measures representing different modes of variability including ENSO (using the NINO3.4 index), SAM (using the SAM index) and IOD (using the DMI index). These correlations are all based on the period from 1979 to 2019, using one value for each summer period (DJF). NINO3.4 and DMI data are attained from the NASA ESRL (https://psl.noaa.gov/gcos_wgsp/Timeseries/) while SAM data are from <https://legacy.bas.ac.uk/met/gjma/sam.html>. Pearson's correlation coefficient, r , is shown with stippling corresponding to statistically significant values at the 95% confidence level (2-tailed).

Additional factors- lightning ignitions as well as fuel load and type

Although the focus here is on extreme fire weather conditions, a brief summary is provided here to note some of the other conditions that are important for the occurrence of bushfires. This includes ignition sources as well as vegetation-related factors such as fuel load and type.

Lightning was the ignition source for many of the largest and most damaging fires during the 2019/2020 summer fire season in southeast Australia (Australian Government 2020). In addition to individual summers, lightning has been found to cause most of the total area burnt when averaged over many fire seasons in southeast Australia (Dowdy & Mills 2012) with lightning-ignited fires also being response for a large amount of the area burnt during the Black Summer (Australian Government 2020). Human-caused ignitions are also a key cause

of fires in Australia, noting that projected future changes in that are highly uncertain. Given the occurrence of lightning, the chance that it will cause a sustained ignition and develop into a bushfire is strongly dependent on the amount of rainfall that accompanies it, leading to the concept of 'dry lightning' as an important natural ignition source for bushfires (i.e., lightning that occurs without significant rainfall). There is some indication of an increased frequency of dry-lightning in some parts of southeast Australia in recent decades as well as decreases in some other regions more broadly for Australia (Dowdy 2020a). However, projections of future changes in the occurrence of dry-lightning is a key knowledge gap in general for Australia, affecting our understanding of potential changes to bushfire ignition and bushfire occurrence throughout Australia.

Changes in vegetation characteristics including amount (fuel load) and type can also influence fire hazards throughout Australia, noting that this is particularly important for grassfires in the more northern and central regions of Australia (McKeon et al. 2009). There are potential increases in fuel loads for various vegetation types associated with projected increases in carbon dioxide concentrations, often referred to as the 'fertilisation effect' (Clarke et al. 2016), where higher concentrations of atmospheric carbon dioxide promote vegetation growth (Donohue et al., 2013). Global drylands have generally been greening over recent decades and the fertilisation effect has been identified as a causal factor in this greening (Burrell et al. 2020). Consequently, an increase in some fuel-related fire risk factors may be considered more likely than a decrease, while noting considerable uncertainties given the relatively limited ability of current climate models to accurately simulate future changes in some risk factors relating to fuel characteristics. Similarly, there are also large uncertainties around potential future changes in fuel type, such as whether or not vegetation may shift to types that tend to burn more frequently during this transition period to a warmer world, with no studies currently available on this topic for Australia.

5.3 Summaries for historical information

Observed trends

Early studies on fire weather trends in Australia based on FFDI were not able to separate the influences, if any, of climate change as different to natural variability such as concluded by Clarke et al. (2013). Using a longer time period, different methods and a gridded analysis based on observations, a statistically significant increase in FFDI has since been documented, particularly during spring and summer in many parts of southern and eastern Australia, with this being attributable at least in part to human-caused climate change including increased temperatures and associated changes in relative humidity and fuel availability indicators (Dowdy 2018). Similar results were also reported based on station data for individual locations, finding that significant increases in FFDI have already occurred during spring and summer different to what can likely be explained based on natural variability alone (Harris & Lucas 2019). Studies using observations-based data and reanalysis have also examined other fire weather indices in Australia, including the C-Haines index over the period back to 1979 (Dowdy & Pepler 2018), finding that statistically significant increases have already occurred including during summer in some parts of southeast Australia, including for simultaneous occurrences of dangerous near-surface and upper-level conditions (based on FFDI and C-Haines). Such results have been confirmed in other recent climate change studies considering a range of factors that can influence fire weather, including some analysis over palaeontological time scales (Abram et al. 2021).

Model assessment

The ability of climate models to simulate aspects such as the seasonal cycle, observed trends, spatial detail and extremes is important for helping to understand the degree of confidence in future projected changes based on these models. Assessments as presented in various studies (CSIRO & BoM 2015; Di Virgilio et al. 2019; Dowdy et al. 2019b) indicate that global models as well as downscaling approaches provide a reasonably good representation of these aspects, including seasonal and regional variations through Australia as well as the observed trends in general towards more dangerous weather conditions for bushfires in Australia.

5.4 Summaries for projected changes

As discussed in sections above, previous studies have examined projected future changes in measures of extreme such as FFDI exceeding 25 or 50 as well as FFDI exceeding its historical 95th or 99th percentile. Here we examine projections of the 10-yr ARI of daily FFDI from the available modelling approaches based on GCMs, CCAM, BARPA and NARCliM. These datasets all have QME calibration applied to the input variables for each individual model prior to calculating the FFDI, with the ARI values then calculated from the FFDI using a GEV approach (as was the case for temperature extremes in Section 3). The results show increases in the severity of fire weather conditions projected from the historical climate to the future projected climate during summer (i.e., December, January and February), as represented by the 10-yr ARI value of daily FFDI. Some variation is apparent between the different model ensembles in the magnitude of the increases, with somewhat larger increases for NARCliM in some regions, but with general agreement over these modelling approaches on a projected future increase in these values corresponding to the 10-year ARI.

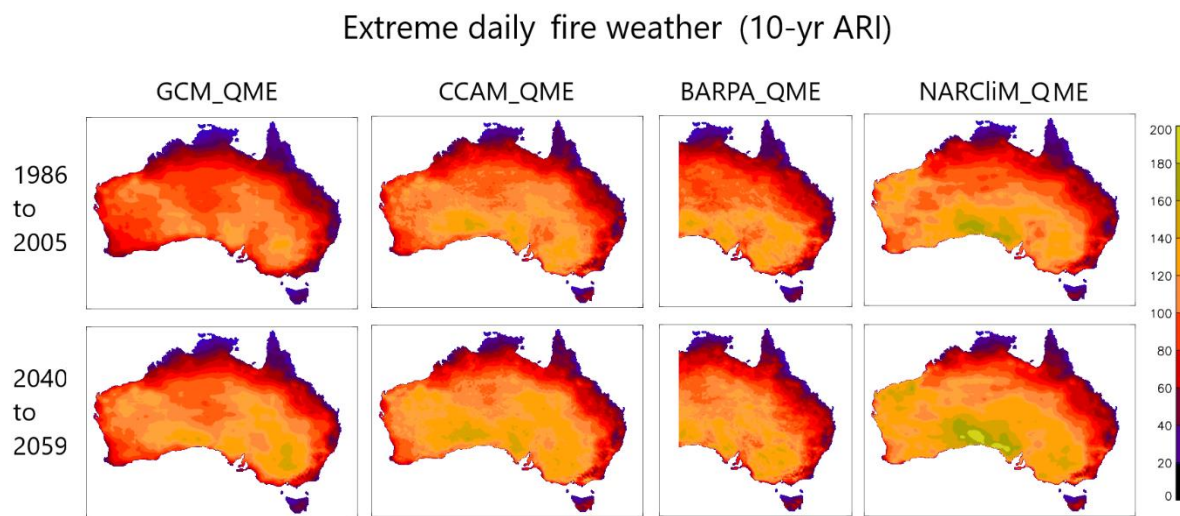


Figure 5.2: Projections for values corresponding to the 10-year ARI for daily fire weather conditions as represented by the FFDI (with the FFDI intended as a useful means of combining different weather factors known to influence fire behaviour in Australia). This is shown based on GCMs (left panels), CCAM (second to left panels), BARPA (second to right panels) and NARCliM (right panels), all calibrated using the QME method. Maps are shown through Australia based on the model ensemble average in each case, presented for the historical period (based on 1986-2005; upper panels) as well as for the future simulated climate (based on 2040-2059 under a high emissions pathway RCP8.5 from CMIP5; lower panels).

5.5 Lines of Evidence Table

Table 5.1: Lines of Evidence Table for extreme fire weather conditions, with a focus on summer in the southeast and east of Australia. The degree of influence is listed in black, followed by whether this information implies an increase (red), decrease (blue) or little change (black) in the frequency and severity of extreme fire weather conditions, as well as by increased uncertainty (purple) in the direction of change. The rows of information are not in order of importance.

Physical processes and their measures	
Individual weather factors	Strong association. More extreme temperatures and heatwaves, lower relative humidity; small decrease in wind speed.
Drought and fuel moisture	Strong association. Projected increase in frequency of meteorological drought and very dry fuel conditions. Reasonable confidence for some contributing factors from global models (but potentially overestimated some conditions and considerable uncertainties for other factors); regional models likely to add value.
Combined near-surface weather conditions, FFDI	Strong association. Projected increase in frequency of dangerous conditions in general based on numerous studies; poor agreement between models near east coast.
Combined near-surface weather conditions, FWI	Strong association. Projected increase, but not statistically significant, and only based on one study.
Upper-level conditions, C-Haines	Strong association (including extreme pyroconvection). Increased frequency of dangerous conditions in southeast (including simultaneous occurrence with dangerous near-surface conditions) and decrease in northeast.
Subtropical ridge	Moderate association in southeast. Potential increase.
Blocking	Moderate association. Future change uncertain.
Fronts	Moderate association. Future change uncertain.
ENSO	Strong association. Uncertain future change; potential increase for ENSO extremes (low confidence).
IOD	Strong association. Uncertain future change; potential increase for IOD extremes (medium confidence).
SAM	Strong association in central east. Positive trend in SAM reducing dangerous fire weather in central east region (medium confidence).
Assessment for historical period	
Seasonal cycle	Models reproduce the seasonal cycle and spatial variability well (high confidence).
Historical trend	Increase from observations (medium confidence). Models reproduce the trend well (medium confidence).
Projected future change	
GCMs	Increase (high confidence).
CCAM	Increase (high confidence in general; medium near east coast).
NARCliM	Increase (high confidence in general; medium near east coast).
BARPA	Increase (high confidence in general). Based on one model to date.
Additional factors	
Lightning ignitions	Strong association. Influence of climate change largely uncertain but increase more likely than decrease (low confidence).
Fuel load and type	Strong association. Influence of climate change largely uncertain but increased fuel load more likely than decrease (low confidence).

5.6 Projections Likelihood Information

The Lines of Evidence Table shows considerable agreement on more dangerous fire weather conditions in a warming climate for Australia, including in relation to 10-year ARI fire weather conditions in the southeast and east of Australia during summer (as is a key focus here). Although there are some physical processes noted that add uncertainties, particularly based on GCM projections data, the RCM approaches can help with the simulation of some of these processes such that the moderate level of agreement between RCM approaches (particularly in southern Australia but somewhat less so in parts of eastern Australia) helps add some confidence for projected future changes. Observed trends and RCM simulations are available for near-surface and higher-level conditions, including combining those different levels using a compound event framework (Dowdy & Pepler 2018; Di Virgilio et al. 2019; Dowdy et al. 2019b), showing increases in southern Australia with more variation between results in eastern Australia including decreases being indicated in some regions. There is low confidence for projected future changes in vegetation-related conditions such as fuel load and type, as well as in ignition risk factors including the occurrence of dry lightning, noting that fuel conditions and ignition sources are important factors for fire occurrence throughout Australia (particularly in many central and northern regions).

Based on this assessment of a broad range of factors that can influence the occurrence of extremely dangerous fire weather conditions, there is *High Confidence* in southern Australia and *Medium Confidence* in parts of eastern Australia for the projected direction of change, with a future increase in 10-year ARI fire weather conditions being *Likely* (i.e., 66-100% probability) for southeastern and eastern Australia. Considering all of the review details in the sections above, and noting the predominance of an increase from the Lines of Evidence Table, projections for 10-year ARI extreme fire weather conditions in 2050 are developed here based on combining data from various calibrated modelling approaches including GCMs (4 ensemble members), CCAM (5 ensemble members), BARPA (1 ensemble member) and NARCliM (6 ensemble members).

FFDI data are available from these models and are the primary data source used here. The contrasting modelling approaches are combined based on equally weighting the changes. The ensemble median is used as a central estimate of the most probable projected change (Figure 5.3). As an estimate of the range of plausible values, the second lowest value from the ensemble is used for the 10th percentile and the second highest value is used from the ensemble is used for the 90th percentile, with these values calculated individually at each grid cell location. However, given some of the uncertainties and variations between different modelling approaches and studies as noted in this section (including projections based on the FWI showing smaller changes than for FFDI), the lower bound of the range provided here has been modified to reflect the potential for lower values. This is done based on reducing any projected increases for the 10th percentile by a factor of two (as a qualitative estimate based on expert judgement). For example, at a given grid-cell location, if the 10th percentile for the future period was higher by a value of 8 as compared to the 1986-2005 value, it would be changed to only be a value of 4 higher than the 1986-2005 value at that location. Projections for any regions that show decreases for the 10th percentile are not changed. Only the 10th percentile is changed to allow for lower values, but no lines of evidence suggest these FFDI projections data systematically underestimate future increases such that the 90th percentile is unchanged and is considered a plausible upper estimate for the future projected changes for these fire weather conditions.

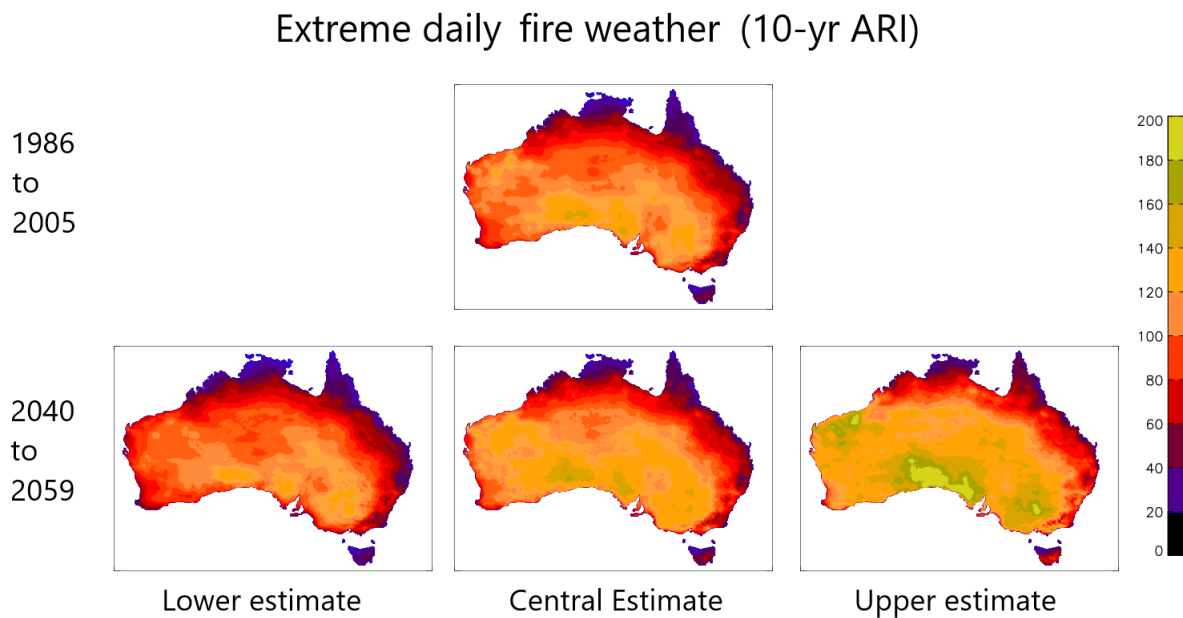


Figure 5.3: Projected change in values corresponding to the 10-year ARI for daily fire weather conditions during summer. Maps are shown through Australia for the historical period (based on 1986-2005; upper panel), as well as for the future simulated climate (based on 2040-2059 under a high emissions pathway RCP8.5: lower panels) including a central estimate with lower and upper estimates also provided. The data are based on the FFDI, with some modifications based on considering the broader lines of evidence from Table 5.1.

6. Conclusion

The influence of climate change on extreme temperatures, winds and fire weather was assessed using a standardised method. This method is based on a review and synthesis of a broad range of information, designed to help guide the production of projections information and confidence assessment. Calibrated data from GCMs and RCMs were used for temperature and fire weather, with environmental diagnostics used for severe convective winds from thunderstorms. The projections presented here are more extreme than examined in previous studies (e.g., 10-yr ARI projections for fire weather and severe convective winds), with care taken to communicate uncertainties and document the comprehensive lines of evidence considered here. Data are available on request.

The nationally consistent calibrated projections presented here, including based on new RCM data from BARPA, CCAM and NARClM as well as GCMs, are intended to be of use for a broad range of applications. This includes for applications such as improved planning and helping to build resilience in relation to the influence of anthropogenic climate change on future hazards in Australia.

References

Abatzoglou, J. T., Williams, A. P., Boschetti, L., Zubkova, M., & Kolden, C. A. (2018). Global patterns of interannual climate–fire relationships. *Global Change Biology*, 24(11), 5164–5175.

Abram, N. J., Henley, B. J., Gupta, A. S., Lippmann, T. J., Clarke, H., Dowdy, A. J., Sharples, J. J., Nolan, R. H., Zhang, T., Wooster, M. J., & Wurtzel, J. B. (2021). Connections of climate change and variability to large and extreme forest fires in southeast Australia. *Communications Earth & Environment*, 2(1), 1–17.

Allen, J., Karoly, D., & Mills, G. (2011). A severe thunderstorm climatology for Australia and associated thunderstorm environments. *Aust. Meteorol. Oceanogr. J.*, 61(3), 143–158.

Allen, J. T., Karoly, D. J., & Walsh, K. J. (2014). Future Australian Severe Thunderstorm Environments. Part I: A Novel Evaluation and Climatology of Convective Parameters from Two Climate Models for the Late Twentieth Century. *J. Clim.*, 27, 3827–3847, doi:10.1175/JCLI-D-13-00425.1

Allen, J. T., Karoly, D. J., & Walsh, K. J. (2014). Future Australian Severe Thunderstorm Environments. Part II: The Influence of a Strongly Warming Climate on Convective Environments. *J. Climate*, 27, 3848–3868.

Allen, J. T., & Karoly, D. J. (2014). A climatology of Australian severe thunderstorm environments 1979 – 2011: Inter-annual variability and ENSO influence. *Int. J. Climatol.*, 34, 81–97.

Allen, J. T., & Allen, E. R. (2016). A review of severe thunderstorms in Australia. *Atmos. Res.*, 178–179, 347–366, doi:10.1016/j.atmosres.2016.03.011

Allen, J. (2018). Climate Change and Severe Thunderstorms. Oxford Research Encyclopedia of Climate Science. Retrieved 13 Jan. 2021, from <https://oxfordre.com/climatescience/view/10.1093/acrefore/9780190228620.001.0001/acrefore-9780190228620-e-62>

Arblaster, J. M., & Alexander, L. V. (2012). The impact of the El Niño–Southern Oscillation on maximum temperature extremes. *Geophysical Research Letters*, 39(20), 2–6, <https://doi.org/10.1029/2012GL053409>

Argüeso, D., Evans, J. P., Fita, L., & Bormann, K. J. (2014). Temperature response to future urbanization and climate change. *Climate Dynamics*, 42(7–8), 2183–2199, <https://doi.org/10.1007/s00382-013-1789-6>

Argüeso, D., Evans, J. P., Pitman, A. J., & Di Luca, A. (2015). Effects of city expansion on heat stress under climate change conditions. *PLoS One*, 10(2), e0117066, doi:10.1371/journal.pone.0117066

Australian Government (2020). Royal Commission into National Natural Disaster Arrangements. Australian Government, ISBN: 978-1-921091-45-2.

Azorin-Molina, C., McVicar, T. R., Guijarro, J. A., Trewin, B., Frost, A. J., Zhang, G., Minola, L., Son, S., Deng, K., & Chen, D. (2021). A decline of observed daily peak wind gusts with distinct seasonality in Australia, 1941-2016, *Journal of Climate*, 1-63. <https://doi.org/10.1175/JCLI-D-20-0590.1>

Banerjee, A., Fyfe, J. C., Polvani, L. M., Waugh, D., & Chang, K. L. (2020). A pause in Southern Hemisphere circulation trends due to the Montreal Protocol. *Nature*, 579(7800), 544–548. <https://doi.org/10.1038/s41586-020-2120-4>

Bates, B. C., Chandler, R. E., & Dowdy, A. J. (2015). Estimating trends and seasonality in Australian monthly lightning flash counts. *Journal of Geophysical Research*, 120(9), 3973–3983. <https://doi.org/10.1002/2014JD023011>

Bell, S. S., Chand, S. S., Tory, K. J., Dowdy, A. J., Turville, C., & Ye, H. (2019). Projections of southern hemisphere tropical cyclone track density using CMIP5 models. *Climate Dynamics*, 52(9), 6065–6079.

Berg, A., Sheffield, J., & Milly, P. C. D. (2017). Divergent surface and total soil moisture projections under global warming. *Geophysical Research Letters*, 44(1), 236–244, <https://doi.org/10.1002/2016GL071921>

Birch, C. E., Roberts, M. J., Garcia-Carreras, L., Ackerley, D., Reeder, M. J., Lock, A. P., & Schiemann, R. (2015). Sea-Breeze Dynamics and Convection Initiation: The Influence of Convective Parameterization in Weather and Climate Model Biases. *Journal of Climate*, 28(20), 8093–8108, <https://doi.org/10.1175/JCLI-D-14-00850.1>

Blázquez, J., & Solman, S. A. (2017). Fronts and precipitation in CMIP5 models for the austral winter of the Southern Hemisphere. *Climate Dynamics*, 50, 2705, <https://doi.org/10.1007/s00382-017-3765-z>

Blázquez, J., & Solman, S. A. (2019). Relationship between projected changes in precipitation and fronts in the austral winter of the Southern Hemisphere from a suite of CMIP5 models. *Climate Dynamics*, 52(9–10), 5849–5860, <https://doi.org/10.1007/s00382-018-4482-y>

Bony, S., et al. (2006). How well do we understand and evaluate climate change feedback processes? *Journal of Climate*, 19, 3445–3482, doi:10.1175/JCLI3819.1

Boschat, G., Pezza, A., Simmonds, I., Perkins, S., Cowan, T., & Purich, A. (2015). Large scale and sub-regional connections in the lead up to summer heat wave and extreme rainfall events in eastern Australia. *Climate Dynamics*, 44(7–8), 1823–1840, <https://doi.org/10.1007/s00382-014-2214-5>

Brooks, H. E., Lee, J. W., & Craven, J. P. (2003). The spatial distribution of severe thunderstorm and tornado environments from global reanalysis data. *Atmospheric Research*, 67–68, 73–94, doi:10.1016/S0169-8095(03)00045-0

Brooks, H. E. (2013). Severe thunderstorms and climate change. *Atmospheric Research*, 123, 129–138, <http://dx.doi.org/10.1016/j.atmosres.2012.04.002>

Brown, A., & Dowdy, A. (2019). Extreme wind gusts and thunderstorms in South Australia analysed from 1979-2017. Bureau Research Report No. 034. Available at: <http://www.bom.gov.au/research/publications/researchreports/BRR-034.pdf> (accessed 25 November 2020).

Brown, A., & Dowdy, A. (2021). Severe convection-related winds in Australia and their associated environments. *Journal of Southern Hemisphere Earth Systems Science*, <https://doi.org/10.1071/ES19052>

Bureau of Meteorology (BOM), & CSIRO (2020). State of the Climate 2020. Available from: <http://www.bom.gov.au/state-of-the-climate/>

Burrell, A. L., Evans, J. P., & De Kauwe, M. G. (2020). Anthropogenic climate change has driven over 5 million km² of drylands towards desertification. *Nature Communications*, 11(1), 1-11.

Cai, W., T. Cowan & M. Raupach (2009). Positive Indian Ocean Dipole events precondition southeast Australia bushfires. *Geophysical Research Letters* 23, 3357-3360. <https://doi.org/10.1029/2009GL039902>

Cai, W., Wang, G., Dewitte, B., Wu, L., Santoso, A., Takahashi, K., Yang, Y., Careric, A., & McPhaden, M. J. (2018a). Increased variability of eastern Pacific El Niño under greenhouse warming. *Nature* 564, 201-206. <https://doi.org/10.1038/s41586-018-0776-9>

Cai, W., Wang, G., Gan, B., Wu, L., Santoso, A., Lin, X., Chen, Z., Jia, F., & Yamagata, T. (2018b): Stabilised frequency of extreme positive Indian Ocean Dipole under 1.5C warming. *Nature Communications*, 9, 1419. <https://doi.org/10.1038/s41467-018-03789-6>

Cai, W., Wu, L., Lengaigne, M., Li, T., McGregor, S., Kug, J.-S., et al. (2019). Pantropical climate interactions. *Science*, 363(6430), eaav4236. <https://doi.org/10.1126/science.aav4236>

Catto, J. L., Nicholls, N., Jakob, C., & Shelton, K. L. (2014). Atmospheric fronts in current and future climates. *Geophysical Research Letters*, 41(21), 7642–7650, <https://doi.org/10.1002/2014GL061943>

Catto, J. L., Jakob, C., & Nicholls, N. (2015). Can the CMIP5 models represent winter frontal precipitation? *Geophysical Research Letters*, 42(20), 2015GL066015, <https://doi.org/10.1002/2015GL066015>

Cechet, R. P., Sanabria, L. A., Divi, C. B., Thomas, C., Yang, T., Arthur, W. C., Dunford, M., Nadimpalli, K., Power, L., White, C. J. & Bennett, J. C. (2012). Climate Futures for Tasmania: severe wind hazard and risk technical report.

Chambers, C. R. S., Brassington, G. B., Walsh, K. et al. (2015). Sensitivity of the distribution of thunderstorms to sea surface temperatures in four Australian east coast lows. *Meteorology and Atmospheric Physics*, 127, 499–517. doi:10.1007/s00703-015-0382-4

Chand, S. S., Dowdy, A. J., Ramsay, H. A., Walsh, K. J., Tory, K. J., Power, S. B., Bell, S. S., Lavender, S. L., Ye, H., & Kuleshov, Y. (2019). Review of tropical cyclones in the Australian region: Climatology, variability, predictability, and trends. *Wiley Interdisciplinary Reviews: Climate Change*, 10(5), p.e602.

Chapman, S., Thatcher, M., Salazar, A., Watson, J. E. M., & McAlpine, C.A. (2019). The impact of climate change and urban growth on urban climate and heat stress in a subtropical city. *International Journal of Climatology*, 39, 3013– 3030. <https://doi.org/10.1002/joc.5998>

Chen, J., Dai, A., Zhang, Y., & Rasmussen, K. L. (2020). Changes in convective available potential energy and convective inhibition under global warming. *Journal of Climate*, 33(6), 2025-2050.

Chew L. W., Liu X., Li X-X, & Norford, L. K. (2020). Interaction between heat wave and urban heat island: A case study in a tropical coastal city, Singapore. *Atmospheric Research*, 247, 105134, <https://doi.org/10.1016/j.atmosres.2020.105134>

Clarke, H., Lucas, C., & Smith, P. (2013). Changes in Australian fire weather between 1973 and 2010. *International Journal of Climatology*, 33(4), 931-944.

Clarke, H., Pitman, A. J., Kala, J., Carouge, C., Haverd, V., & Evans, J. (2016). An investigation of future fuel load and fire weather in Australia. *Climatic Change*, 139 (3), 591-605.

Clarke, H., & Evans, J. P. (2019). Exploring the future change space for fire weather in southeast Australia. *Theoretical and Applied Climatology*, 136(1), 513-527.

Clemesha, R. E. S., Guirguis, K., Gershunov, A., Small, I. J., & Tardy, A. (2018). California heat waves: their spatial evolution, variation, and coastal modulation by low clouds. *Climate Dynamics*, 50, 4285–4301, <https://doi.org/10.1007/s00382-017-3875-7>

Cruz, M. G., Sullivan, A. L., Gould, J. S., Sims, N. C., Bannister, A. J., Hollis, J. J., & Hurley, R. J. (2012). Anatomy of a catastrophic wildfire: the Black Saturday Kilmore East fire in Victoria, Australia. *Forest Ecology and Management*, 284, 269–285.

CSIRO & Bureau of Meteorology (2015). Climate Change in Australia Information for Australia's Natural Resource Management Regions: Technical Report, CSIRO and Bureau of Meteorology, Australia.

Dawson, A., Palmer, T. N., & Corti, S. (2012) Simulating regime structures in weather and climate prediction models. *Geophysical Research Letters*, 39, L21805, doi:10.1029/2012GL053284

Di Virgilio, G., Evans, J. P., Blake, S. A., Armstrong, M., Dowdy, A. J., Sharples, J., & McRae, R. (2019). Climate change increases the potential for extreme wildfires. *Geophysical Research Letters*, 46(14), 8517–8526.

Diffenbaugh, N. S., M. Scherer, & R. J. Trapp (2013). Robust increases in severe thunderstorm environments in response to greenhouse forcing. *Proceedings of the National Academy of Sciences*, 110, 16361–16366, doi:10.1073/pnas.1307758110

Donohue, R. J., M. L. Roderick, T. R. McVicar, & G. D. Farquhar (2013). Impact of CO₂ fertilization on maximum foliage cover across the globe's warm, arid environments, *Geophysical Research Letters*, 40, 3031–3035, doi:10.1002/grl.50563

Doswell, C. A., & Evans, J. S. (2003). Proximity sounding analysis for derechos and supercells: An assessment of similarities and differences. *Atmospheric Research*, 67–68, 117–133.

Dowdy, A. J., Mills, G. A., Finkele, K., & de Groot, W. (2009). Australian fire weather as represented by the McArthur forest fire danger index and the Canadian forest fire weather index. Centre for Australian Weather and Climate Research Tech. Rep, 10, p.91.

Dowdy, A. J., & Mills, G. A. (2012). Atmospheric and fuel moisture characteristics associated with lightning-attributed fires. *Journal of Applied Meteorology and Climatology*, 51(11), 2025–2037.

Dowdy, A. J. (2014). Long-term changes in Australian tropical cyclone numbers. *Atmospheric Science Letters*, 15(4), 292–298.

Dowdy, A., Grose, M., Timbal, B., Moise, A., Ekstrom, M., Bhend, J., & Wilson, L. (2015). Rainfall in Australia's eastern seaboard: a review of confidence in projections based on observations and physical processes. *Australian Meteorological and Oceanographic Journal*, 65(1), 107–126. <https://doi.org/10.22499/2.6501.008>

Dowdy, A. J. (2016). Seasonal forecasting of lightning and thunderstorm activity in tropical and temperate regions of the world. *Scientific Reports*, 6, 1–10, doi:10.1038/srep20874

Dowdy, A. J., & J. L. Catto (2017). Extreme weather caused by concurrent cyclone, front and thunderstorm occurrences. *Scientific Reports*, 1–8, doi:10.1038/srep40359

Dowdy, A. J., Fromm, M. D., & McCarthy, N. (2017). Pyrocumulonimbus lightning and fire ignition on Black Saturday in southeast Australia. *Journal of Geophysical Research: Atmospheres*, 122(14), 7342–7354.

Dowdy, A. J. (2018). Climatological variability of fire weather in Australia. *Journal of Applied Meteorology and Climatology*, 57(2), 221–234.

Dowdy, A. J., & Pepler, A. (2018). Pyroconvection risk in Australia: Climatological changes in atmospheric stability and surface fire weather conditions. *Geophysical Research Letters*, 45(4), 2005–2013.

Dowdy, A. J., Pepler, A., Di Luca, A., Cavigchia, L., Mills, G., Evans, J., et al. (2019a). Review of Australian east coast low pressure systems and associated extremes. *Climate Dynamics*, 53, 4887, [https://doi.org/https://doi.org/10.1007/s00382-019-04836-8](https://doi.org/10.1007/s00382-019-04836-8)

Dowdy, A. J., Ye, H., Pepler, A., Thatcher, M., Osbrough, S. L., Evans, J. P., Di Virgilio, G., & McCarthy, N. (2019b). Future changes in extreme weather and pyroconvection risk factors for Australian wildfires. *Scientific Reports*, 9(1), 1-11.

Dowdy, A. J. (2020a). Climatology of thunderstorms, convective rainfall and dry lightning environments in Australia. *Climate Dynamics*, doi:10.1007/s00382-020-05167-9

Dowdy, A. J. (2020b). Seamless climate change projections and seasonal predictions for bushfires in Australia. *Journal of Southern Hemisphere Earth Systems Science*, 70(1), 120-138.

Drobinski, P., Bastin, S., Arsouze, T. et al. (2018). North-western Mediterranean sea-breeze circulation in a regional climate system model. *Climate Dynamics*, 51, 1077–1093. <https://doi.org/10.1007/s00382-017-3595-z>

Fasullo, J. T., Otto-Bliesner, B. L., & Stevenson, S. (2018). ENSO's Changing Influence on Temperature, Precipitation, and Wildfire In a Warming Climate. *Geophysical Research Letters*, 1–10, <https://doi.org/10.1029/2018GL079022>

Field, R. D., Spessa, A. C., Aziz, N. A., Camia, A., Cantin, A., Carr, R., De Groot, W. J., Dowdy, A. J., Flannigan, M. D., Manomaiphiboon, K., & Pappenberger, F. (2015). Development of a global fire weather database. *Natural Hazards and Earth System Sciences*, 15(6), 1407-1423.

Fischer, E. M., Oleson, K. W., and Lawrence, D. M. (2012). Contrasting urban and rural heat stress responses to climate change, *Geophysical Research Letters*, 39, L03705, doi:10.1029/2011GL050576

Fita L., Evans, J. P., Argüeso, D., King, A., & Liu, Y. (2016). Evaluation of the regional climate response in Australia to large-scale climate modes in the historical NARClM simulations. *Climate Dynamics*, 1–15, <https://doi.org/10.1007/s00382-016-3484-x>

Freund, M. B., Brown, J. R., Henley, B. J., Karoly, D. J., & Brown J. N. (2020). Warming patterns affect El Nino diversity in CMIP5 and CMIP6 models. *Journal of Climate*, 10.1175/JCLI-D-19-0890.1

Fromm, M., Tupper, A., Rosenfeld, D., Servranckx, R., & McRae, R. (2006). Violent pyro-convective storm devastates Australia's capital and pollutes the stratosphere. *Geophysical Research Letters*, 33(5).

Garfinkel, C. I., Waugh, D. W., & Polvani, L. M. (2015). Recent Hadley cell expansion: The role of internal atmospheric variability in reconciling modeled and observed trends. *Geophysical Research Letters*, 42(24), 10824–10831, <https://doi.org/10.1002/2015GL066942>

Gartland, L. (2011). Heat Islands: Understanding and mitigating heat in urban areas. Routledge. ISBN 9781849712989

Gensini, V. A., Ramseyer, C., & Mote, T. L. (2014). Future convective environments using NARCCAP. *International Journal of Climatology*, 34, 1699–1705, doi:10.1002/joc.3769

Gensini, V. A., & Brooks, H. E. (2018). Spatial trends in United States tornado frequency. *npj Climate and Atmospheric Science*, 1(1), 1-5. <https://doi.org/10.1038/s41612-018-0048-2>

Gibson, P. B., Perkins-Kirkpatrick, S. E., Uotila, P., Pepler, A. S., & Alexander, L. V. (2017). On the use of self-organizing maps for studying climate extremes. *Journal of Geophysical Research*, 122(7), 3891–3903, <https://doi.org/10.1002/2016JD026256>

Grise, K. M., Davis, S. M., Simpson, I. R., Waugh, D. W., Fu, Q., Allen, R. J., et al. (2019). Recent tropical expansion: Natural variability or forced response? *Journal of Climate*, 32(5), 1551–1571, <https://doi.org/10.1175/JCLI-D-18-0444.1>

Grise, K. M., & Polvani, L. M. (2014). Southern Hemisphere Cloud–Dynamics Biases in CMIP5 Models and Their Implications for Climate Projections. *Journal of Climate* 27, 15, 6074–6092, <https://doi.org/10.1175/JCLI-D-14-00113.1>

Grose, M., Timbal, B., Wilson, L., Bathols, J., & Kent, D. (2015). The subtropical ridge in CMIP5 models, and implications for projections of rainfall in southeast Australia. *Australian Meteorological and Oceanographic Journal*, 65, 90–106, <https://doi.org/10.22499/2.6501.007>

Gross, M. H., Donat, M. G., & Alexander, L. V. (2019). Changes in daily temperature extremes relative to the mean in CMIP5 models and observations. *International Journal of Climatology*, (October 2018), 1–19, <https://doi.org/10.1002/joc.6138>

Grose, M. R., Narsey, S., Delage, F. P., Dowdy, A. J., Bador, M., Boschat, G., Chung, C., Kajtar, J. B., Rauniyar, S., Freund, M. B., & Lyu, K. (2020). Insights from CMIP6 for Australia's future climate. *Earth's Future*, 8(5), p.e2019EF001469.

Guan, H., Kumar, V., Clay, R., Kent, C., Bennett, J., Ewenz, C., Hopkins, G., & Simmons, C. T. (2016). Temporal and spatial patterns of air temperature in a coastal city with a slope base setting. *Journal of Geophysical Research: Atmospheres*, 121(10): 2016JD025139, <https://doi.org/10.1002/2016JD025139>

Harris, S., & Lucas, C. (2019). Understanding the variability of Australian fire weather between 1973 and 2017. *PloS One*, 14(9), p.e0222328.

Hasson, A. E. A., Mills, G. A., Timbal, B., & Walsh, K. (2009). Assessing the impact of climate change on extreme fire weather events over southeastern Australia. *Climate Research*, 39(2), 159–172, <https://doi.org/10.3354/cr00817>

Hendon, H. H., Thompson, D. W. J., & Wheeler, M. C. (2007). Australian rainfall and surface temperature variations associated with the Southern Hemisphere annular mode. *Journal of Climate*, 20(11), 2452–2467, <https://doi.org/10.1175/JCLI4134.1>

Hersbach, H., Bell, B., Berrisford, P., Hirahara, S., Horányi, A., et al. (2020). The ERA5 global reanalysis. *Quarterly Journal of the Royal Meteorological Society*, 146(730), 1999–2049.

Herold, N., Kala, J., & Alexander, L. V. (2016). The influence of soil moisture deficits on Australian heatwaves. *Environmental Research Letters*, 11(6), <https://doi.org/10.1088/1748-9326/11/6/064003>

Hirsch, A. L., Evans, J. P., Di Virgilio, G., Perkins-Kirkpatrick, S. E., Argüeso, D., Pitman, A. J., et al. (2019). Amplification of Australian Heatwaves via Local Land-Atmosphere Coupling. *Journal of Geophysical Research: Atmospheres*, 625–647, <https://doi.org/10.1029/2019JD030665>

Holmes, J. D. (2002). A Re-analysis of Recorded Extreme Wind Speeds in Region A. *Australian Journal of Structural Engineering*, 4, 29–40, doi:10.1080/13287982.2002.11464905

Holmes, J. D. (2020) Land-falling tropical cyclones on the Queensland coast and implications of climate change for wind loads, *Australian Journal of Structural Engineering*, 21, 135–142, DOI: 10.1080/13287982.2020.1717842

Hoogewind, K. A., Baldwin, M. E., & Trapp, R. J. (2017). The Impact of Climate Change on Hazardous Convective Weather in the United States: Insight from High-Resolution Dynamical Downscaling, *Journal of Climate*, 30(24), 10081–10100.

Hope, P., Grose, M. R., Timbal, B., Dowdy, A. J., Bhend, J., Katzfey, J. J., et al. (2015). Seasonal and regional signature of the projected southern Australian rainfall reduction. *Australian Meteorological and Oceanographic Journal*, 65(1), 54–71, <https://doi.org/10.22499/2.6501.005>

Imran, H. M., Kala, J., Ng, A. W. M. & Muthukumaran, S. (2019). Impacts of future urban expansion on urban heat island effects during heatwave events in the city of Melbourne in southeast Australia. *Quarterly Journal of the Royal Meteorological Society*, 145, 2586–2602, <https://doi.org/10.1002/qj.3580>

IPCC (2013). Climate Change 2013: The Physical Science Basis. Contribution of Working Group I to the Fifth Assessment Report of the Intergovernmental Panel on Climate Change [Stocker, T.F., D. Qin, G.-K. Plattner, M. Tignor, S.K. Allen, J. Boschung, A. Nauels, Y. Xia, V. Bex & P.M. Midgley (eds.)]. Cambridge University Press, Cambridge, United Kingdom and New York, NY, USA, 1535 pp.

Jakob, D. (2010). Challenges in developing a high-quality surface wind-speed data-set for Australia. *Australian Meteorological and Oceanographic Journal*, 60, 227-236, 10.22499/2.6004.001.

Jovanovic, B., Jones, D. A., & Collins, D. (2008). A high-quality monthly pan evaporation dataset for Australia. *Clim. Change*, 87, 517–35.

Keetch, J. J., & Byram, G. M. (1968). A drought index for forest fire control. USDA Forest Service, Research Paper SE-38.

Kendon, E. J., et al. (2017). Do convection-permitting regional climate models improve projections of future precipitation change? *Bulletin of the American Meteorological Society*, 98, 79–93, doi:10.1175/BAMS-D-15-0004.1

Kent, D. M., Kirono, D. G. C., Timbal, B., & Chiew, F. H. S. (2013). Representation of the Australian sub-tropical ridge in the CMIP3 models. *International Journal of Climatology*, 33(1), 48–57, <https://doi.org/10.1002/joc.3406>

King, A. T., & A. D. Kennedy (2019). North American supercell environments in atmospheric reanalyses and RUC-2. *Journal of Applied Meteorology and Climatology*, 58, 71–92, doi:10.1175/JAMC-D-18-0015.1

Knutson, T., Camargo, S. J., Chan, J. C., Emanuel, K., Ho, C. H., Kossin, J., Mohapatra, M., Satoh, M., Sugi, M., Walsh, K., & Wu, L. (2020). Tropical cyclones and climate change assessment: Part II: Projected response to anthropogenic warming. *Bulletin of the American Meteorological Society*, 101(3), E303-E322.

Kuchera, E. L. & Parker, M. D. (2006). Severe Convective Wind Environments. *Weather Forecasting*, 21(4), 595–612.

Leslie, L. M., Leplastrier, M., & Buckley, B. W. (2008). Estimating future trends in severe hailstorms over the Sydney Basin: A climate modelling study. *Atmospheric Research*, 87, 37–51.

Lim, E.-P., Hendon, H. H., Arblaster, J. M., Delage, F., Nguyen, H., Min, S.-K., & Wheeler, M. C. (2016). The impact of the Southern Annular Mode on future changes in Southern Hemisphere rainfall. *Geophysical Research Letters*, 2016GL069453, <https://doi.org/10.1002/2016GL069453>

Lim, E.-P., Hendon, H. H., Boschat, G., Hudson, D., Thompson, D. W. J., Dowdy, A. J., & Arblaster, J. M. (2019). Australian hot and dry extremes induced by weakenings of the stratospheric polar vortex. *Nature Geoscience*, 12(11), 896–901, <https://doi.org/10.1038/s41561-019-0456-x>

Lim, E. P., Hendon, H. H., Butler, A. H., Thompson, D. W., Lawrence, Z., Scaife, A. A., Shepherd, T. G., Polichtchouk, I., Nakamura, H., Kobayashi, C., & Comer, R. (2021). The 2019 Southern Hemisphere stratospheric polar vortex weakening and its impacts. *Bulletin of the American Meteorological Society*, 1-50.

Loughran, T. F., Pitman, A. J., & Perkins-Kirkpatrick, S. E. (2019). The El Niño–Southern Oscillation's effect on summer heatwave development mechanisms in Australia. *Climate Dynamics*, 52(9–10), 6279–6300. <https://doi.org/10.1007/s00382-018-4511-x>

Lucas, C., (2010). A High-quality Historical Humidity Database for Australia. CAWCR Technical Report 24, Bureau of Meteorology, Docklands, Victoria, Australia.

Maloney, E. D., Adames, Á. F., & Bui, H. X. (2019). Madden–Julian oscillation changes under anthropogenic warming. *Nature Climate Change*, 9(1), 26–33, <https://doi.org/10.1038/s41558-018-0331-6>

Marjani, S., Alizadeh-Choobari, O., & Irandejad, P. (2019). Frequency of extreme El Niño and La Niña events under global warming. *Climate Dynamics*, 53(9), 5799–5813, <https://doi.org/10.1007/s00382-019-04902-1>

Marshall, A. G., Hudson, D., Wheeler, M. C., Alves, O., Hendon, H. H., Pook, M. J., & Risbey, J. S. (2013). Intra-seasonal drivers of extreme heat over Australia in observations and POAMA-2. *Climate Dynamics*, 43(7–8), 1915–1937, <https://doi.org/10.1007/s00382-013-2016-1>

Marshall, G. J. (2003). Trends in the Southern Annular Mode from observations and reanalyses. *Journal of Climate*, 16(24), 4134–4143, [https://doi.org/10.1175/1520-0442\(2003\)016<4134:TITSAM>2.0.CO;2](https://doi.org/10.1175/1520-0442(2003)016<4134:TITSAM>2.0.CO;2)

Masouleh, Z. P., Walker, D. J., & McCauley Crowther, J. (2019). A Long-Term Study of Sea-Breeze Characteristics: A Case Study of the Coastal City of Adelaide, *Journal of Applied Meteorology and Climatology*, 58(2), 385–400.

Mastrandrea, M. D., et al. (2011). The IPCC AR5 guidance note on consistent treatment of uncertainties: a common approach across the working groups. *Climatic Change*, 108(4), 675–691.

McArthur, A. G. (1967). Fire behaviour in eucalypt forests. Forestry and Timber Bureau, No 107, Canberra, Australia.

McKeon, G. M., et al. (2009). Climate change impacts on northern Australian rangeland livestock carrying capacity: a review of issues, *Rangel. J.*, 31, 1–29.

McRae, R. H., Sharples, J. J., Wilkes, S. R., & Walker, A. (2013). An Australian pyro-tornadogenesis event. *Natural Hazards*, 65(3), 1801–1811.

McVicar, T. R., Van Niel, T. G., Li, L. T., Roderick, M. L., Rayner, D. P., Ricciardulli, L., & Donohue, R. J. (2008). Wind speed climatology and trends for Australia, 1975–2006: Capturing the stilling phenomenon and comparison with near-surface reanalysis output. *Geophysical Research Letters*, 35(20), L20403, <https://doi.org/10.1029/2008GL035627>

Mills, G. A., & McCaw, W. L. (2010). Atmospheric stability environments and fire weather in Australia: extending the Haines Index. CAWCR Technical Report, Centre for Australia and Weather Climate Research, Melbourne, Australia.

Myers, T. A., & Norris, J. R. (2015). On the Relationships between Subtropical Clouds and Meteorology in Observations and CMIP3 and CMIP5 Models. *Journal of Climate* 28, 8, 2945–2967, <https://doi.org/10.1175/JCLI-D-14-00475.1>

NESP (2020). Earth Systems and Climate Change Hub. 2020. Scenario analysis of climate-related physical risk for buildings and infrastructure: climate science guidance. Technical report by the National Environmental Science Program (NESP) Earth Systems and Climate Change Science (ESCC) Hub for the Climate Measurement Standards Initiative, ESCC Hub Report No.21, ISBN: 978-0-6489444-1-6.

Nguyen, H., Lucas, C., Evans, A., Timbal, B., & Hanson, L. (2015). Expansion of the Southern Hemisphere Hadley cell in response to greenhouse gas forcing. *Journal of Climate*, 28(20), 8067–8077, <https://doi.org/10.1175/JCLI-D-15-0139.1>

Parker, T. J., Berry, G. J., & Reeder, M. J. (2013). The influence of tropical cyclones on heatwaves in Southeastern Australia. *Geophysical Research Letters*, <https://doi.org/10.1002/2013GL058257>

Parker, T. J., Berry, G. J., Reeder, M. J., & Nicholls, N. (2014). Modes of climate variability and heat waves in Victoria, southeastern Australia. *Geophysical Research Letters*, 41(19), 6926–6934, <https://doi.org/10.1002/2014GL061736>

Patterson, M., Bracegirdle, T., & Woollings, T. (2019). Southern Hemisphere atmospheric blocking in CMIP5 and future changes in the Australia-New Zealand sector. *Geophysical Research Letters*, 5, 1–10, <https://doi.org/10.1029/2019gl083264>

Pepler, A. S., Alexander, L. V., Evans, J. P., & Sherwood, S. C. (2015). Zonal winds and southeast Australian rainfall in global and regional climate models. *Climate Dynamics*, 46, 123–133, <https://doi.org/10.1007/s00382-015-2573-6>

Pepler, A. S., Di Luca, A., Ji, F., Alexander, L. V., Evans, J. P., & Sherwood, S. C. (2016). Projected changes in east Australian midlatitude cyclones during the 21st century. *Geophysical Research Letters*, 43, 334–340, doi:10.1002/2015GL067267

Pepler, A., Ashcroft, L., & Trewin, B. (2018). The relationship between the subtropical ridge and Australian temperatures. *Journal of Southern Hemisphere Earth Systems Science*, 68(1), 201–214, <https://doi.org/10.22499/3.6801.011>

Pepler, A. S., Dowdy, A. J., & Hope, P. (2021). The differing role of weather systems in southern Australian rainfall between 1979 – 1996 and 1997 – 2015. *Climate Dynamics*, <https://doi.org/10.1007/s00382-020-05588-6>

Perkins, S. E., Argüeso, D., & White, C. J. (2015). Relationships between climate variability, soil moisture, and Australian heatwaves. *Journal of Geophysical Research: Atmospheres*, 120(16), 2015JD023592, <https://doi.org/10.1002/2015JD023592>

Perkins-Kirkpatrick, S. E., White, C. J., Alexander, L. V., Argüeso, D., Boschat, G., Cowan, T., et al. (2016). Natural hazards in Australia: heatwaves. *Climatic Change*, 139(1), 101–114. <https://doi.org/10.1007/s10584-016-1650-0>

Pistotnik, G., P. Groenemeijer, & R. Sausen (2016). Validation of Convective Parameters in MPI-ESM Decadal Hindcasts (1971-2012) against ERA-Interim Reanalyses. *Meteorologische Zeitschrift*, 25, 753–766, doi:10.1127/metz/2016/0649.

Power, S., Casey, T., Folland, C., Colman, A., & Mehta, V. (1999). Inter-decadal modulation of the impact of ENSO on Australia. *Climate Dynamics*, 15(5), 319–324.

Power, S. B., & Callaghan, J. (2016). Variability in severe coastal flooding, associated storms, and death tolls in Southeastern Australia since the mid-nineteenth century. *Journal of Applied Meteorology and Climatology*, 55(5), 1139–1149, <https://doi.org/10.1175/JAMC-D-15-0146.1>

Proctor, F. H. (1989). Numerical simulations of an isolated microburst. Part II: sensitivity experiments. *Journal of the Atmospheric Science*, 46, 2143–2165

Púčik, T., et al. (2017). Future changes in European severe convection environments in a regional climate model ensemble. *Journal of Climate*, 30, 6771–6794, doi:10.1175/JCLI-D-16-0777.1

Purich, A., Cowan, T., Cai, W., van Rensch, P., Uotila, P., Pezza, A., et al. (2014). Atmospheric and Oceanic Conditions Associated with Southern Australian Heat Waves: A CMIP5 Analysis. *Journal of Climate*, 27(20), 7807–7829, <https://doi.org/10.1175/JCLI-D-14-00098.1>

Quinting, J. F., & Reeder, M. J. (2017). Southeastern Australian Heat Waves from a Trajectory Viewpoint. *Monthly Weather Review*, 145(10), 4109–4125, <https://doi.org/10.1175/MWR-D-17-0165.1>

Quinting, J. F., Parker, T. J., & Reeder, M. J. (2018). Two Synoptic Routes to Subtropical Heat Waves as Illustrated in the Brisbane Region of Australia. *Geophysical Research Letters*, 700–708, <https://doi.org/10.1029/2018GL079261>

Rädler, A. T., Groenemeijer, P., Faust, E., & Sausen, R. (2018). Detecting severe weather trends using an additive regressive convective hazard model (AR-CHaMo). *Journal of Applied Meteorology and Climatology*, 57(3), 569–587.

Rasmussen, K. L., A. F. Prein, R. M. Rasmussen, K. Ikeda, & C. Liu (2017). Changes in the convective population and thermodynamic environments in convection-permitting regional climate simulations over the United States. *Climate Dynamics*, 0, 1–26, <http://dx.doi.org/10.1007/s00382-017-4000-7>

Raupach, T. H., Martius, O., Allen, J. T., Kunz, M., Lasher-Trapp, S., Mohr, S., Rasmussen, K. L., Trapp, R. J. and Zhang, Q. (2021). The effects of climate change on hailstorms. *Nature Reviews Earth & Environment*, 1-14.

Reeder, M. J., Spengler, T., & Musgrave, R. (2015). Rossby waves, extreme fronts, and wildfires in southeastern Australia. *Geophysical Research Letters*, 42(6), 2015-2023.

Rogers, C. D. W., Gallant, A. J. E., & Tapper, N. J. (2019). Is the urban heat island exacerbated during heatwaves in southern Australian cities? *Theoretical and Applied Climatology*, 137(1), 441–457, <https://doi.org/10.1007/s00704-018-2599-x>

Rudeva, I., & Simmonds, I. (2015). Variability and trends of global atmospheric frontal activity and links with large-scale modes of variability. *Journal of Climate*, 28(8), 3311–3330, <https://doi.org/10.1175/JCLI-D-14-00458.1>

Schwalm, C. R., Glendon, S., & Duffy, P. B. (2020). RCP8.5 tracks cumulative CO₂ emissions. *Proceedings of the National Academy of Sciences*, 117(33), 19656-19657.

Scott, A. A., Waugh D. W., & Zaitchik, B. F. (2018). Reduced Urban Heat Island intensity under warmer conditions. *Environmental Research Letters*, 13, 064003, <https://doi.org/10.1088/1748-9326/aabd6c>

Seeley, J. T., & Romps, D. M. (2015). The effect of global warming on severe thunderstorms in the United States. *Journal of Climate*, 28, 2443–2458, doi:10.1175/JCLI-D-14-00382.1

Smith, B. T., Castellanos, T. E., Winters, A. C., Mead, C. M., Dean, A. R., & Thompson, R. L. (2012). Measured Severe Convective Wind Climatology and Associated Convective Modes of Thunderstorms in the Contiguous United States, 2003–09. *Weather Forecasting*, 28(1), 229–236.

Soderholm, J. S., H. McGowan, H. Richter, K. Walsh, T. M. Weckwerth, & M. Coleman (2017). An 18-year climatology of hailstorm trends and related drivers across southeast Queensland, Australia. *Quarterly Journal of the Royal Meteorological Society*, 143, 1123–1135, doi:10.1002/qj.2995

Spassiani, A. C. (2020) Climatology of severe convective wind gusts in Australia (PhD. thesis). The University of Queensland School of Civil Engineering, doi: 10.14264/uql.2020.901

Taszarek, M., Brooks, H. E., & Czernecki, B. (2017). Sounding-Derived Parameters Associated with Convective Hazards in Europe. *Monthly Weather Review*, 145, 1511–1528, doi:10.1175/MWR-D-16-0384.1

Taszarek, M., Allen, J., Brooks, H., Pilguy, N., & Czernecki, B. (2020). Differing trends in United States and European severe thunderstorm environments in a warming climate. *Bulletin of the American Meteorological Society*, 1–51, doi:10.1175/BAMS-D-20-0004.1

Taylor, K. E., Stouffer, R. J. & Meehl, G. A, (2012). An Overview of CMIP5 and the experiment design. *Bull. Amer. Met. Soc.*, 93, 485-498, <https://doi.org/10.1175/BAMS-D-11-00094.1>

Thatcher, M. et al. (2021). Technical Report on downscaling for the ESCI project. Available from ESCI project website.

Timbal, B., & Drosdowsky, W. (2013). The relationship between the decline of Southeastern Australian rainfall and the strengthening of the subtropical ridge. *International Journal of Climatology*, 33(4), 1021–1034, <https://doi.org/10.1002/joc.3492>

Trapp, R. J., N. S. Diffenbaugh, H. E. Brooks, M. E. Baldwin, E. D. Robinson, & J. S. Pal (2007). Changes in severe thunderstorm environment frequency during the 21st century caused by anthropogenically enhanced global radiative forcing. *Proceedings of the National Academy of Science*, 104, 19719–19723, doi:10.1073/pnas.0705494104

Trapp, R. J., K. A. Hoogewind, & S. Lasher-Trapp (2019). Future changes in hail occurrence in the United States determined through convection-permitting dynamical downscaling. *Journal of Climate*, 32, 5493–5509, doi:10.1175/JCLI-D-18-0740.1

Ukkola, A. M., Pitman, A. J., Donat, M. G., De Kauwe, M. G., & Angélil, O. (2018). Evaluating the Contribution of Land-Atmosphere Coupling to Heat Extremes in CMIP5 Models. *Geophysical Research Letters*, 45(17), 9003–9012, <https://doi.org/10.1029/2018GL079102>

Ukkola, A. M., Roderick, M. L., Barker, A., & Pitman, A. J. (2019). Exploring the stationarity of Australian temperature, precipitation and pan evaporation records over the last century. *Environmental Research Letters*, 14(12), p.124035.

Ukkola, A. M., De Kauwe, M. G., Roderick, M. L., Abramowitz, G., & Pitman, A. J. (2020). Robust future changes in meteorological drought in CMIP6 projections despite uncertainty in precipitation. *Geophysical Research Letters*, 47(11), p.e2020GL087820.

van Oldenborgh, G. J., Krikken, F., Lewis, S., Leach, N. J., Lehner, F., Saunders, K. R., van Weele, M., Haustein, K., Li, S., Wallom, D. and Sparrow, S. (2021). Attribution of the Australian bushfire risk to anthropogenic climate change. *Natural Hazards and Earth System Sciences*, 21(3), 941-960.

Van Wagner, C. E. (1974). Structure of the Canadian forest fire weather index, Vol. 1333, Ontario: Environment Canada, Forestry Service.

Voigt, A., Albern, N., Ceppi, P., Grise, K., Li, Y., & Medeiros, B. (2020). Clouds, radiation, and atmospheric circulation in the present-day climate and under climate change. *Wiley Interdisciplinary Reviews: Climate Change*, p.e694.

Walsh, K., et al. (2016). Natural hazards in Australia: storms, wind and hail. *Climate Change*, 139, 55–67, doi:10.1007/s10584-016-1737-7

Wang, C., Wang, X. & Khoo, Y. B. (2013). Extreme wind gust hazard in Australia and its sensitivity to climate change. *Nat. Hazards*, 67, 549–567, DOI:10.1007/s11069-013-0582-5

Wang, G., & Cai, W. (2013). Climate-change impact on the 20th-century relationship between the Southern Annular Mode and global mean temperature. *Scientific Reports* 3, 2039, <https://doi.org/10.1038/srep02039>

Wang, B., Chen, G. & Liu, F. (2019). Diversity of the Madden-Julian Oscillation. *Science Advances*, 5, eaax0220. <https://doi.org/10.1126/sciadv.aax0220>

Waugh, D. W., Garfinkel, C. I., & Polvani, L. M. (2015). Drivers of the recent tropical expansion in the southern hemisphere: Changing SSTs or ozone depletion? *Journal of Climate*, 28(16), 6581–6586, <https://doi.org/10.1175/JCLI-D-15-0138.1>

Wehrli, K., Guillod, B. P., Hauser, M., Leclair, M., & Seneviratne, S. I. (2019). Identifying key driving processes of recent heatwaves and droughts, 21, 13643, <https://doi.org/10.1029/2019JD030635>

Williams, S., Nitschke, M., Sullivan, T., Tucker, G. R., Weinstein, P., Pisaniello, L., Parton, K. A., & Bi, P. (2012). Heat and health in Adelaide, South Australia: Assessment of heat thresholds and temperature relationships. *Science of the Total Environment*, 414, 126–133, <https://doi.org/10.1016/j.scitotenv.2011.11.038>

Woollings, T., Barriopedro, D., Methven, J., Son, S. W., Martius, O., Harvey, B., et al. (2018). Blocking and its Response to Climate Change. *Current Climate Change Reports*, <https://doi.org/10.1007/s40641-018-0108-z>

Wouters, H., et al. (2017). Heat stress increase under climate change twice as large in cities as in rural areas: A study for a densely populated midlatitude maritime region, *Geophysical Research Letters*, 44, 8997–9007, doi:10.1002/2017GL074889

Zhao, L., Oppenheimer, M., Zhu, Q., Baldwin, J. W., Ebi, K. L., Bou-Zeid, E., Guan, K., & Liu, X. (2018). Interactions between urban heat islands and heat waves. *Environmental Research Letters*, 13, 034003, <https://doi.org/10.1088/1748-9326/aa9f73>